Population burdens of air pollution around the world: Distributions, inequalities, and links to per capita GDP

Preliminary draft

The latest version of this paper is available at this link.

Angelo Santos, Oscar Morales, Jere Behrman, Emily Hannum, Fan Wang*

March 17, 2024

Abstract

We analyze the global population-weighted distribution of air pollution by aerosols and its relationship to GDP per capita. We first decompose the global distribution and consider both variations across and within regions and countries. Second, we map national and subnational distributions of air pollution by aerosols to national and subnational distributions of GDP per capita. We find considerable global exposure inequalities. Comparing continents at the extremes, the average individual in Asia is 3.32 times more exposed to air pollution by aerosols than the average individual in Oceania. In Africa and Asia, populations at the 80^{th} percentile of the air pollution by aerosol distribution are 141% and 109% more exposed than population at the 20^{th} percentile, and those at the 90^{th} percentile are 227% and 185% more exposed those at the 10^{th} percentile. Globally, we find that a doubling of GDP per capita is associated with a 11.8 percentage points reduction in the percentage deviation between a subnational unit's population-weighted air pollution by aerosol level and the global population-weighted mean. Within each continent, exploiting variabilities in subnational data after controlling for aggregate regional variabilities, we find positive associations between air pollution by aerosols and GDP per capita in Africa and Europe, but negative association in the Americas, Asia, and Oceania.

*Angelo Santos: Department of Economics, University of Houston, Houston, Texas, USA; Oscar Morales: Department of Economics, University of Houston, Houston, Texas, USA; Jere Behrman: Department of Economics and Sociology, University of Pennsylvania, Philadelphia, PA 19104, USA; Emily Hannum: Department of Sociology and Population Studies Center, University of Pennsylvania, PA, USA; Fan Wang: Department of Economics, University of Houston, Houston, Texas, USA. This paper is part of the project "Climate Risk, Pollution, and Childhood Inequalities in Low- and Middle-income Countries," which is supported by National Science Foundation Grant 2230615 (PI: Hannum)

1 Introduction

Air-pollution exposure has been increasing over time and growing evidence has pointed to this exposure as a high-risk factor for global health (Gakidou et al. 2017). Fine-particulate-matter exposure, especially from $PM_{2.5}$, has been indicated as the cause of millions of deaths in the world, and negatively correlated with outcomes such as health, children's cognitive development, and productivity (Fisher et al. 2021; Fu, Viard, and Zhang 2021; Odo et al. 2023). Additionally, more than half of the global population is exposed to shallow quality air (PM2.5 concentration of more than $\mu g/m^3$) and this exposure has been increasing over time (Pirlea and Huang 2019; Shaddick et al. 2020). In light of this, it is important to understand what is the global distribution of air pollution across and within countries better understand the global population risks of air pollution.

A large literature documents changing patterns of global climatic and pollution exposures, however, the scientific literature generally focuses on variations in climatic measures across locations and time, without tying the data to the geographical distribution of the population experiencing these changes (Mehta et al. 2016; Tian et al. 2023). In social science, there is also a rapidly growing empirical literature that uses available micro-data from parts of the world to estimate the effects of pollution exposures on labor market productivity, health, as well as educational outcomes (Brabhukumr et al. 2020; Gakidou et al. 2017; Odo et al. 2023). These papers, however, do not provide global analyses of the overall pollution burdens facing population from across the world.

This paper contributes to burgeoning literature that combines global population distribution and global air pollutant measurements to study global heterogeneities in population-weighted air pollution burden (Shaddick et al. 2018; Van Donkelaar et al. 2021). Prior papers in this literature have generally focused on comparing regional and national mean measures. Our paper is the first to analyze inequalities in air pollution distributions across and within regions and countries of the world. We accomplish this by decomposing the global population-weighted air pollution distribution into across and within region and country components.

Additionally, we provide the first global analysis that maps global national and subnational variations in air pollution to economic development as captured by GDP per capita. We provide results on the direction and magnitude of the GDP per capita and air pollution association globally and for each continent, and use continental and regional fixed effects to explain

whether aggregate associations are due to across region or within region variabilities.

Our analysis is based on gridded high-resolution global data on pollution and population and subnational GDP per capita data from around 2010, the year around which globally reliable measures of air pollution, population and GDP are available. For air pollution, we use data on air pollution by aerosols, as captured by satellite-based Aerosol Optical Depth (AOD) measurements (Xiong et al. 2020). We combine the air pollution by aerosol data with gridded granular national population census and population register data (CIESIN Columbia University 2018). We compute in particular the relative burden of air pollution by aerosol facing population in a particular gridded cell versus the global population-weighted mean exposure, and we construct country-specific population distributions of air pollution burden based on the geographical dispersion of population and air pollution within each country. Finally, we combine the population-weighted air pollution data, aggregated to subnational levels, with subnational GDP per capita data (Gennaioli et al. 2013; Kummu, Taka, and Guillaume 2018).

We find considerable global inequalities in population-weighted air pollution by aerosol exposures. Population in Asia, the continent with the highest level of air pollution by aerosols, face a mean exposure level that is 3.3 times larger than those faced by population in Oceania, which has the lowest mean exposure among continents. Looking across regions within continents, we find that in Eastern Asia, the subcontinental region with the highest level of air pollution by aerosols, population face a mean exposure level that is 6.0 times larger than that faced by population in Australia and New Zealand, which have the lowest mean exposure among subcontinental regions,

In terms of inequalities, across continents, population at the 80^{th} percentile of the continental air pollution by aerosol distribution have between 28% (Europe) to 141% (Africa) greater air pollution by aerosol exposures than population at the 20^{th} percentile. Across subcontinental regions, population at the 80^{th} percentile of the regional air pollution by aerosol distribution have between 2% to 208% greater air pollution by aerosol exposures than population at the 20^{th} percentile. Within countries, population at the 80^{th} percentile of country-specific air pollution by aerosol distributions have between 0% to 359% greater air pollution by aerosol exposures than population at the 20^{th} percentile.

For the global GDP per capita and air pollution by aerosol analysis, overall, we find a strong negative global correlation. This indicates that globally, national and subnational economic units with higher GDP per capita tend to have lower air pollution by aerosols. Specifically, us-

ing subnational population-weighted data, we find that a doubling of GDP per capita is associated with a 11.8 percentage points reduction in the percentage deviation between a subnational unit's population-weighted air pollution by aerosol level and the global population-weighted mean. This global association is largely explained by correlation between continental-level mean GDP per capita and air pollution by aerosol.

Furthermore, we analyze the GDP and air pollution relationship within each continent. Exploiting variabilities in subnational data after controlling for aggregate regional variabilities, we find a positive association between air pollution by aerosols and GDP per capita in Africa and Europe, but negative association in the Americas, Asia, and Oceania.

2 Data and Methods

2.1 Data and aggregation

Air pollution by aerosols as measured by AOD Aerosols are ensembles of suspended particles present in the Earth's atmosphere. Atmospheric pollution by aerosols is important to human health and well-being because higher amounts of aerosol particles degrade visibility and can also damage health, especially when there is a higher concentration of $PM_{2.5}$ particles that are smaller then 2.5 micrometers (Jacobson 2002). Aerosol Optical Depth (AOD) is a satellite-based measure that captures the composition, sizes and concentration of aerosols by measuring the magnitudes atmospheric light reflection and absorption across the globe (Lenoble, Remer, and Tanre 2013). Scaled between 0 to 1, an AOD value that is less than 0.1 indicates crystal clear sky and clear satellite to earth surface visibility. In contrast, a AOD value close to 1 indicates very hazy conditions (NASA Earth Observatory 2024).

We use AOD measurements based on images collected by the TERRA satellite with its MODIS instruments (Xiong et al. 2020), and we access the data via the NASA EarthData data collection and using the OpenDAP protocol (Cornillon, Gallagher, and Sgouros 2003). On each day in a particular year, tracking along TERRA's orbital path across the globe, we download AOD data at a spatial resolution of 3km $\times$ 3km and at all available 5 minute temporal resolution units. For each day, this process generates a vector of latitude-, longitude-, and time-specific AOD measurements.

Within each $1^\circ \times 1^\circ$ longitude–latitude grid (cell), we compute average daily AOD values based on the subset of the daily AOD measurement vector that fall within the geographical

boundaries of each cell on that day. Repeating this across days during a year, we generate for each cell, a vector of average daily AOD measurements. During each year, the length of these cell-specific daily average AOD vectors is equal to the number of days in which valid AOD measurements are available for a particular cell. On some days, there might be no cell-specific AOD measurements due to high cloud fraction and invalid reflectance assumptions (Wang et al. 2021) or due to limited overlaps between the cells and the daily orbital path (Xiong et al. 2020).

Using the cell-specific vectors of average daily AOD measurements from a year, we compute annual average AOD exposures for each cell, first averaging over the days in which cell-specific measurements are available, and then separately averaging over all days after complementing the observed averages with interpolated and extrapolated estimates on days without cell-specific measurements. Due to the concentration of missing AOD data in regions with the least population, our population-weighted AOD distributional results based on the raw data and interpolated and extrapolated data are very similar. Our global inequality results presented in the text are based on annual averages of the raw data.[1]

Global gridded population data In conjunction with the cell-specific AOD data, we generate cell-specific global population estimates based on the Gridded Population of the World Version 4 (GPWv4) dataset from the Center for International Earth Science Information Network (CIESIN Columbia University 2018). The GPWv4 data contains population statistics from 241 global economies. Data is sourced in most cases from national and local statistical agencies, and when that is not available, sourced from the United Nations.

The gridded GPWv4 data provides total population estimates at 30 arc-second grids ($\sim$ 1km at the equator), and is aggregated based on up to administrative level 6 population data from global economies. For example, the gridded data is aggregated from population data from 316,461 Brazilian sectors, 43,878 Chinese townships, 5,967 Indian sub-districts, 774 Nigerian local government areas, and 10,535,212 US census blocks. To allow for the calculation population-weighted AOD data, we aggregate the GPWv4 population estimates up to $1^\circ \times 1^\circ$ longitude–latitude grid, which matches up with the resolution of our cell-specific annual average AOD exposures data.

Due to variabilities in census survey and population register data availability, GPWv4 pop-

1. See Appendix Figure C.1 for a visualization of the number of days in 2010 with AOD measurements across global cells.

ulation data are sourced between the years 2001 and 2015, with the center of the calendar year distribution at around 2010. Specifically, data from 27% of the economies are based on 2010 census and population register data, 62% and 83% of the economies' data come from within one and three years of 2010, and about 8% of the economies have data sourced from outside of four years of 2010. To appropriately match up the time-frame of the population and AOD data, we use cell-specific annual average AOD exposure data in 2010.

Subnational GDP data We complement global measurements of air pollution by aerosols and population with data on the relative levels of economic development as captured by GDP per capita. Specifically, we use national and subnational from the Gridded global datasets for Gross Domestic Product (Kummu, Taka, and Guillaume 2018), which is based on subnational GDP per capita data from Gennaioli et al. (2013). The GDP per capita values are adjusted for purchasing price parity and based on 2005 international dollars.

Gennaioli et al. (2013) collected subnational GDP data from 1569 subnational first-level or equivalent administrative units from the largest 110 economies up to 2010. These economies accounted for 97% of global GDP in 2010. Kummu, Taka, and Guillaume (2018) augmented the dataset with national GDP data from economies without subnational data, filled in missing subnational GDP values by interpolating based on geographically and temporally neighboring data-points around missing values, and extended the dataset time-frame to 2015 by extrapolating based on trends up to 2010.

Considering jointly the temporal availability of AOD, pollution, and GDP data, we use the 2010 subnational and national GDP per capita estimates from Kummu, Taka, and Guillaume (2018).

2.2 Population weighted distributional statistics for AOD

Population-weighted AOD distributions To analyze population-weighted air pollution by aerosol distributions, we define a discrete distribution of 2010 annual average AOD values over the set of all populated cells, where the cell-specific population mass is determined by GPWv4-based population estimates from around 2010. Specifically, let s_c be the share of global population in cell c, a_c be the average annual AOD at cell c, and C be the set of all gridded cells where $s_c > 0$. The global population-weighted annual average AOD distribution function, which provides the share of global population experiencing lower than a^* levels of annual

average AOD, is equal to:

$$F(a^*) = P(a < a^*) = \sum_{c \in C} s_c \cdot \mathbf{1}\{a_c < a^*\} \ . \tag{1}$$

To compare aerosol distributions conditional on regional groupings based on supranational, national, and subnational boundaries, we define $C_r \subseteq C$ as the set of populated cells that intersect with the boundary enclosures of supranational, national, or subnational location r. For boundary data, we use national boundary data available in the GPWv4 population dataset (CIESIN Columbia University 2018), and the subnational boundary data embedded in the subnational GDP data from (Kummu, Taka, and Guillaume 2018). The share of population in cell c conditional on location grouping r is $s_{c,r} = \frac{s_c}{(\sum_{\hat{c} \in C_r} s_{\hat{c}})}$, and the locational AOD distribution function is:

$$F_r(a^*) = P_r(a < a^*) = \sum_{c \in C_r} s_{c,r} \cdot \mathbf{1}\{a_c < a^*\} \ . \tag{2}$$

Given the locational distribution function, we compute key distributional statistics for each location r. The mean and variance of the location r-specific distributions are

$$\begin{aligned} \mu_r &= \sum_{c \in C_r} s_{c,r} \cdot a_c \\ \text{and } \sigma_r^2 &= \sum_{c \in C_r} s_{c,r} \cdot (a_c - \mu_r)^2 \ . \end{aligned} \tag{3}$$

The global weighted mean is $\mu_{\text{global}} = \sum_{c \in C} s_c \cdot a_c$. In our empirical analysis, we compute global, continental, regional, national, and subnational population weighted annual mean AOD exposures.

Given the discrete mass distribution over cells, the location distribution function $F_r(a^*)$ is not invertible. Hence, we define the τ^{th} percentile of the locational distribution as the minimum a^* value where the share of population in location r with less than a^* level of annual average AOD is greater or equal to $\frac{\tau}{100}$, specifically:

$$\text{percentile}_r(\tau) = \min \left\{ a^* : F_r(a^*) \geqslant \frac{\tau}{100} \right\} \ . \tag{4}$$

Discussions in our empirical analysis focus on location-specific 20^{th} and 80^{th} as well as 10^{th} and 90^{th} percentiles, and use relative percentile ratios as an additional measures for within location

distributional variabilities.

Relative exposure and excess burden To measure relative exposures, we compute what we call excess aerosol burden, $e_{c,\widehat{r}}$, which is the percentage deviation between cell-specific AOD value a_c and location-specific AOD value average $\mu_{\widehat{r}}$:

$$e_{c,\widehat{r}} = \frac{a_c - \mu_{\widehat{r}}}{\mu_{\widehat{r}}} = \frac{a_c}{\mu_{\widehat{r}}} - 1 \ . \tag{5}$$

When $\widehat{r}$ includes all global cells, we have $e_{c,\text{global}}$, the global excess aerosol burden. We also divide weighted mean from location r against that of another location $\widehat{r}$:

$$e_{r,\widehat{r}} = \frac{\mu_r - \mu_{\widehat{r}}}{\mu_{\widehat{r}}} = \frac{\mu_r}{\mu_{\widehat{r}}} - 1 \ . \tag{6}$$

When r is a country and $\widehat{r}$ includes all global cells, $e_{\text{country,global}}$ is the country-specific excess aerosol burdens relative to the global mean. A global excess aerosol value of 0 indicates that a location has the same AOD measure as the global mean, and a value of 0.5 or -0.5 indicates that a location's AOD measure is 50 percent greater or smaller than the global mean.

As an additional interpretation of the ratio of the weighted means of a subset over a superset, $e_{r,\text{global}}$ can also be expressed as:

$$e_{r,\text{global}} = \frac{\overbrace{\left(\frac{\left(\sum_{c \in C_r} s_c\right) \cdot \mu_r}{\mu_{\text{global}}}\right)}^{\text{Location } r \text{ pop-weighted pollution share}}}{\underbrace{\left(\sum_{c \in C_r} s_c\right)}_{\text{Location } r \text{ population share}}} - 1 = \frac{\mu_r}{\mu_{\text{global}}} - 1 \ . \tag{7}$$

A value of 0.5 or -0.5 for $e_{r,\text{global}}$ indicates that location r's share of global population-weighted air pollution is 50 percent greater or smaller than location r's share of global population.

AOD and $PM_{2.5}$ As a satellite-based measure of air pollution by aerosols, AOD measurements increase with greater concentrations of atmospheric particles, including $PM_{2.5}$ particles. While our analysis is focused on the distribution of air pollution by aerosols as measured by AOD, to help provide additional interpretation of our AOD results, in our presentation and discussion of results, we provide results both in AOD as well as in estimated AOD-transformed $PM_{2.5}$ scales.

While AOD captures directly visibility experiences, the best-fitting model that maps between atmospheric aerosol measurements and on-the-ground ambient particulate matter exposure experienced by people is parameterized by heterogeneous topological and meteorological circumstances (Chu et al. 2016; Holben et al. 1998; Van Donkelaar et al. 2016; Yang et al. 2019). Overall, atmospheric-based AOD measures have been found to substantively and positively correlate with ground-based aerosol and $PM_{2.5}$ measurements (Bibi et al. 2015; Bright and Gueymard 2019; Chu et al. 2016), and AOD is often used as a predictor of ambient $PM_{2.5}$ exposures with locally and temporally calibrated prediction functions (Chen et al. 2022; Fu et al. 2018; Yang et al. 2019).

To create a globally consistent and transparent scale, we use a global linear model to relate our AOD estimates to existing global estimates of $PM_{2.5}$. Specifically, we relate the cell-specific annual average AOD values we derived to global gridded estimates of surface $PM_{2.5}$ concentration derived based on models that use satellite-based AOD measures as inputs and ground-based $PM_{2.5}$ data for calibration and model validation (Hammer et al. 2020). Regressing the $PM_{2.5}$ values from Hammer et al. (2020) on our AOD measures, we find that a bivariate linear model provides a reasonable global fit with an R^2 of 0.4. We obtain similar fit and estimates when we restrict the data to only populated cells or when we use all available cells, and higher polynomial orders do not significantly improve the fit.

In our results discussions, we also compare the AOD-transformed $PM_{2.5}$ measures to the WHO interim targets for particulate matter air pollution.[2] These targets are used as guidelines for classifying the severity of $PM_{2.5}$ exposures. The WHO guideline recommends lowering annual average exposure levels to less than $35\,\mu g/m^3$, $25\,\mu g/m^3$, $15\,\mu g/m^3$, and $10\,\mu g/m^3$ as interim targets 1, 2, 3, and 4.

3 Within and across country distributions of air pollution by aerosols

Combining global AOD measures and population data, we present in this section the overall population-weighted global distribution of air pollution by aerosols. In contrast to prior studies on global population-based inequality in ambient air pollution, which have focused on comparing means across regions and countries (Shaddick et al. 2018; Van Donkelaar et al. 2021; Van Donkelaar et al. 2016), we study global inequalities based by conducting comparisons

2. The report can be found here https://www.who.int/publications/i/item/9789240034228

within and across region as well as countries.

3.1 Global distributions

Overall global distribution Figure 1 presents histograms for the global relative distribution of air pollution by aerosols, measured in units of excess aerosol burden. The country-based result in Panel (a) shows the country-aggregate population weighted distribution of country-specific within-country population-weighted means. The cell-based distribution in Panel (b) uses cell-specific results, weighted by cell-specific population estimates.[3]

Panel (a)'s country-level distribution of global excess aerosol burden ranges from -0.81 to 1.18, and has an 80^{th} percentile that is 1.44 times larger relative to its 20^{th} percentile. In contrast, Panel (b)'s cell level distribution of global excess aerosol burden ranges from approximately -1.0 to 10.06, and has an 80^{th} percentile that is 3.62 times more exposed than the 20^{th} percentile. Comparisons between the panels demonstrate that country-level information, even when properly weighted by within country distributions, masks the inequalities across cells within countries. Our analysis in the following sections focus on population-weighted cell-based distributions.

Global dispersion map Figure 2 presents a global map of the relative distribution of air pollution by aerosols in Panel (a). The map matches cell-specific AOD to cell locations. The colors correspond to levels of global excess aerosol burdens—darker shades of green (red) represent greater magnitudes of negative (positive) excess burdens.

The map shows that Asia and Africa have relatively higher levels of air pollution by aerosols. Focusing on countries, India, China, and Pakistan stand out as large countries with areas experiencing high levels of excess aerosol burdens. In contrast, Australia, Mexico, and Argentina are also large economies, but have relatively lower levels of excess aerosol burdens. Additionally, there are variations in the within-country heterogeneities of exposures. For example, locations in the southeastern and northwestern regions of China have high excess burdens, but areas in northern and southwestern China have relative lower levels of excess burdens. In contrast, countries within Western Europe and North America tend to have limited variations concentrated around lower levels of excess burdens.

While the world map provides a useful visualization of the global dispersion of air pollu-

3. In Appendix Figure C.2, we present un-weighted histograms.

tion, it does not show the relative population shares facing these heterogeneous burdens across locations.

Population-weighted distributions across continents In Panel (b) of Figure 2, we present continent-specific air pollution distributions that combine the distributions of population and excess aerosol burdens across cells.

Comparing continents at the extremes, the average individual in Asia is 3.32 times more exposed to air pollution by aerosols than the average individual in Oceania. Asia and Oceania have average excess burdens of 0.26 ($\approx$ 29.10 $\mu g/m^3$ of $PM_{2.5}$) and -0.63 ($\approx$ 8.76 $\mu g/m^3$ of $PM_{2.5}$). This means that Asia's and Oceania's global shares of air pollution by aerosols are 26% larger and 63% smaller than their global population shares.

Africa is has the second highest mean exposure with a approximate average $PM_{2.5}$ value of 19.91 $\mu g/m^3$, followed by Europe and the Americas at 14.32 $\mu g/m^3$ and 12.11 $\mu g/m^3$. Oceania is the only continent with average $PM_{2.5}$ reaching WHO interim target 4, which suggests that a considerable share of the world lives in places where air pollution by aerosol exposures are above recommended healthy condition levels.

In addition to the means, the Panel (b) of Figure 2 also shows heterogeneities in the population-weighted dispersion of excess aerosol burdens within each continent. The Americas, Europe, and Oceania have distributions with relatively limited variabilities. Europe is the most equal continent in the world where population at the 80^{th} percentile of excess aerosol burden are only 28% more exposed than those at the 20^{th} percentile. In contrast, distributions in Africa and Asia are more dispersed. Populations at the 80^{th} percentile of the aerosol distribution are 141% and 109% more exposed than population at the 20^{th} percentile in Africa and Asia, respectively. Further at the tails, the exposure faced by populations at the 90^{th} percentile of the aerosol distribution are 227% and 185% higher than those at the 10^{th} percentile in Africa and Asia, respectively.

3.2 Distributions across and within regions and countries

In this section, we decompose the global air pollution by aerosol distribution into sub-continental region- and nation-specific components. We present the results in continent-specific Figures 3 to 6. In each figure, Panel (a) presents air pollution by aerosol distributions by sub-continental group (e.g., Northern Africa, East Asia), and Panel (b) highlights the 20^{th} and 80^{th} percentiles

and means of country-specific distributions. Both results are based on population-weighted cell-level results.

There are substantial differences in means and variabilities across sub-continental regions. In terms of means, Eastern Asia has the highest mean AOD of 0.66 ($\approx 33.68\,\mu g/m^3$ of $PM_{2.5}$), which is just below WHO interim target 1. Australia and New Zealand have the lowest mean AOD of 0.11 ($\approx 7.65\,\mu g/m^3$ of $PM_{2.5}$), which has reached WHO interim target 4. In terms of variabilities, the ratios of exposure for population at the 80^{th} to 20^{th} percentiles for sub-continental regions range between 1.02 to 3.08, and the 90^{th} to 10^{th} percentile ratios range between 1.06 to 4.31.

Inequalities within Africa Figure 3 shows air pollution by aerosol distributions for countries in Eastern, Middle, Northern, Southern, and Western Africa. Results show substantial heterogeneities in within-region aerosol exposures.

Western Africa has the highest average annual AOD at 0.51 ($\approx 26\,\mu g/m^3$ of $PM_{2.5}$), almost reaching WHO interim target 2. Southern Africa has the lowest average annual AOD at 0.14 ($\approx 9.05\,\mu g/m^3$ of $PM_{2.5}$), which exceeds WHO interim target 4.

The most populous African country, Nigeria, has an annual average AOD of 0.56 ($\approx 28.98\,\mu g/m^3$ of $PM_{2.5}$), which is behind WHO interim target 2. Nigeria's average exposure level corresponds to a global excess aerosol burden of 0.24, meaning that Nigeria's global share of air pollution by aerosols is 24% larger than its population share. Exposure inequalities are significant within Nigeria—Nigerian population at the 80^{th} (90^{th}) percentile of aerosol distribution are 77% (106%) more exposed than those at the 20^{th} (10^{th}) percentile. One of the least populous countries in Africa, Sao Tome and Principe, has an average annual AOD of 0.47 ($\approx 24.65\,\mu g/m^3$ of $PM_{2.5}$), just passing WHO interim target 2. In contrast to Nigeria, relative population exposure percentiles are close to 1 due to the small size of the country.

At 0.66 ($\approx 35.18\,\mu g/m^3$ of $PM_{2.5}$), Congolese population face the highest average annual AOD in Africa, which lags behind WHO interim target 1. Congo's global share of air pollution by aerosols is 53% larger than its population share. Exposure inequalities are limited within Congo—Congolese population at the 80^{th} (90^{th}) percentile of aerosol distribution are 15% (22%) more exposed than those at the 20^{th} (10^{th}) percentile. In contrast, at 0.09 ($\approx 6.42\,\mu g/m^3$ of $PM_{2.5}$), population in Lesotho face the lowest average annual AOD in Africa, which surpasses significantly WHO interim target 4. Lesotho's global share of air pollution by aerosols is 81%

smaller than its population share. Exposure inequalities are limited except at the end tails within Lesotho—Lesothoan population at the 80^{th} (90^{th}) percentile of aerosol distribution are 0% (40%) more exposed than those at the 20^{th} (10^{th}) percentile.

Inequalities within Americas Figure 4 shows air pollution by aerosol distributions for countries in the Caribbean, Central America, Northern America, and South America. Compared to Africa and Asia, distributions in regions in the Americas have limited variabilities.

South America has the highest average annual AOD at 0.22 ($\approx 12.93\,\mu g/m^3$ of $PM_{2.5}$). Central America has the lowest average annual AOD at 0.19 ($\approx 11.65\,\mu g/m^3$ of $PM_{2.5}$). All regions in the Americas, on average, have reached WHO interim targets 3.

The most populous country in the Americas, the United States of America, has an annual average AOD of 0.19 ($\approx 11.67\,\mu g/m^3$ of $PM_{2.5}$), close to reach WHO interim target 4. The US's average exposure level corresponds to a global excess aerosol burden of -0.56, meaning that the US's global share of air pollution by aerosols is 56% smaller than its population share. Exposure inequalities are important but limited in the US—Americans population at the 80^{th} (90^{th}) percentile of aerosol distribution are 36% (71%) more exposed than those at the 20^{th} (10^{th}) percentile. One of the least populous countries in the Americas, Saint Lucia, has an average annual AOD of 0.21 ($\approx 12.49\,\mu g/m^3$ of $PM_{2.5}$). Relative population exposure percentiles is equal to 1 in Saint Lucia.

At 0.34 ($\approx 18.55\,\mu g/m^3$ of $PM_{2.5}$), Colombian population face the highest average annual AOD in the Americas, which is behind WHO interim target 3. Colombia's global share of air pollution by aerosols is 24% smaller than its population share. Exposure inequalities are important but limited within Colombia—Colombian population at the 80^{th} (90^{th}) percentile of aerosol distribution are 28% (55%) more exposed than those at the 20^{th} (10^{th}) percentile. In contrast, at 0.10 ($\approx 7.27\,\mu g/m^3$ of $PM_{2.5}$), population in Chile face the lowest average annual AOD in the Americas, which achieves WHO interim target 4. Chile's global share of air pollution by aerosols is 77% smaller than its population share.

Inequalities within Asia Figure 5 shows air pollution by aerosol distributions for countries in Central, Eastern, Southeastern, Southern, and Western Asia. Results show substantial heterogeneities in within-region and within-country aerosol exposures.

Eastern Asia has both the highest average levels of exposure and variabilities in expo-

sures, and Central Asian has the lowest. Eastern Asia has an average annual AOD of 0.66 ($\approx$ 33.68 $\mu g/m^3$ of $PM_{2.5}$). Eastern Asian population at the 80^{th} percentile of aerosol distribution are 158% more exposed than those at the 20^{th} percentile, and its population at the 90^{th} percentile of aerosol distribution are 223% more exposed than those at the 10^{th} percentile. Central Asia has an average annual AOD of 0.36 ($\approx$ 19.49 $\mu g/m^3$ of $PM_{2.5}$), reaching WHO interim target 3. Central Asia's population at the 80^{th} (90^{th}) percentile of aerosol distribution are 64% (110%) more exposed than those at the 20^{th} (10^{th}) percentile.

The most populous Asian country, China, has an annual average AOD of 0.7 ($\approx$ 35.58 $\mu g/m^3$ of $PM_{2.5}$), which is behind WHO interim target 1, indicating very hazardous levels of average air pollution by aerosols. China's average exposure level corresponds to a global excess aerosol burden of 0.55, meaning that China's global share of air pollution by aerosols is 55% larger than its population share. Exposure inequalities are large within China—Chinese population at the 80^{th} (90^{th}) percentile of aerosol distribution are 111% (216%) more exposed than those at the 20^{th} (10^{th}) percentile. One of the least populous countries in Asia, Qatar, has an average annual AOD of 0.60, which is similar to the level in China. Relative population exposure percentiles are equal to 1 due to the geographical confines of Qatar.

In Asia, populations in Kuwait and East Timor are at the opposite ends of the air pollution by aerosol exposure spectrum. Both countries' relative within country exposure percentiles are close to 1. At 0.99 ($\approx$ 49.06 $\mu g/m^3$ of $PM_{2.5}$), Kuwaiti population face the highest average annual AOD in Asia, which is substantially behind WHO interim target 1. In contrast, at 0.17 ($\approx$ 10.74 $\mu g/m^3$ of $PM_{2.5}$), East Timor population have the lowest average annual AOD in Asia, which almost achieved WHO interim target 4. In terms of global excess aerosol burdens, Kuwait's share of global ambient air pollution by aerosol is 118% larger than its global population share, and East Timor's air pollution share is 60% less than its population share.

Inequalities within Europe Figure 6 shows air pollution by aerosol distributions for countries in Eastern, Northern, Southern, and Western Europe. Compared to Africa and Asia, distributions in European regions have limited variabilities.

Eastern Europe has the highest average annual AOD at 0.28 ($\approx$ 15.53 $\mu g/m^3$ of $PM_{2.5}$), just reaching WHO interim target 3. Southern Europe has the lowest average annual AOD at 0.21 ($\approx$ 12.51 $\mu g/m^3$ of $PM_{2.5}$), exceeding interim target 3.

The most populous European country, Russia, has an annual average AOD of 0.29 ($\approx$

16.39 $\mu g/m^3$ of $PM_{2.5}$), which is behind WHO interim target 3. Russia's average exposure level corresponds to a global excess aerosol burden of -0.34, meaning that Russia's global share of air pollution by aerosols is 34% smaller than its population share. Exposure inequalities are significant within Russia—Russian population at the 80^{th} (90^{th}) percentile of aerosol distribution are 67% (130%) more exposed than those at the 20^{th} (10^{th}) percentile. One of the least populous countries in Europe, Iceland, has an average annual AOD of 0.21 ($\approx$ 12.68 $\mu g/m^3$ of $PM_{2.5}$), close to reaching WHO interim target 4. Despite its limited population, there are exposure variabilities in Iceland due to its large geography—Icelandic population at the 80^{th} (90^{th}) percentile of aerosol distribution are 39% (49%) more exposed than those at the 20^{th} (10^{th}) percentile.

Russia has the highest average annual AOD in Europe. In contrast, at 0.15, population in Norway face the lowest average annual AOD in Europe. Norway's global share of air pollution by aerosols is 65% smaller than its population share. Exposure inequalities are limited but present in Norway—Norwegian population at the 80^{th} (90^{th}) percentile of aerosol distribution are 21% (31%) more exposed than those at the 20^{th} (10^{th}) percentile.

Inequalities within Oceania Figure 7 shows air pollution by aerosol distributions for countries in Oceania, which has a small number of countries dominated in population by Australia, Papua New Guinea, and New Zealand. Melanesia has the highest average annual AOD at 0.20 ($\approx$ 12 $\mu g/m^3$ of $PM_{2.5}$), which is just above WHO interim target 4. As a region, Australia and New Zealand have the lowest average annual AOD at 0.11 ($\approx$ 7.65 $\mu g/m^3$ of $PM_{2.5}$), which exceeds WHO interim target 4. Compared to the rest of the world, all populated cells in Oceania have relative low levels of air pollution by aerosol exposures.

4 Air pollution by aerosols and GDP per capita

In this section we analyze the national and subnational level relationships between air pollution by aerosols, as measured by AOD, and economic development, as measured by GDP (PPP-adjusted) per capita (Gennaioli et al. 2013; Kummu, Taka, and Guillaume 2018). Specifically, we regress GDP per capita on global excess aerosol burdens at the national and subnational levels. We allow for homogeneous or heterogeneous bivariate relationships across continents and account for continental and sub-continental regional fixed effects. We present

our results in Table 1 and Figure 8. Results from various estimations jointly inform the direction and magnitude of the GDP and aerosol association globally and for each continent, and explain whether the findings are due to across region—variations in regional means—or within region—variations in national and subnational values conditional on regional means—associations.

Global association In this section, we analyze the global association between air pollution by aerosols and GDP per capita. We find a strong negative association using both national and subnational data, which are largely explained by associations of continental means.

In Table 1, the global country-level result from column (1) of Panel (a) presents the slope from a bivariate regression of excess aerosol burden on GDP per capita, treating each country with equal weight. We find an estimated slope of -0.075 (s.e. 0.018). This means that a doubling of GDP per capita is associated with reducing a country's excess aerosol burden by 7.5 percentage points—this is a 7.5 percentage points reduction in the percentage deviation between the country-specific AOD value the the global mean. In column (2) of Panel (a), we incorporate in country-specific weights, which leads to a doubling of the slope coefficient to -0.144 (s.e. 0.023). This means that countries with larger population tend to have a stronger negative aerosol to GDP associations.

Given the large heterogeneities in within country air pollution by aerosol distribution as well as large heterogeneities in economic development within countries, patterns based on national aggregates might differ from subnational results. In columns (4) and (5) of Panel (a), we estimate the same relationships as in columns (1) and (2) of Panel (a), but using more granular subnational data. We find similar negative slopes of -0.083 (s.e. 0.007) and -0.118 (s.e. 0.008) from the equal weight and population-weighted results.

In both national and subnational regressions, variations in global GDP per capita explain a significant proportion of variabilities in excess aerosol burden. From the national results, for the unweighted and weighted regressions, 9% and 19% of the variabilities in air pollution by aerosols are accounted for by variabilities in GDP per capita, respectively. For subnational results, the shares of variabilities explained are still substantially at 4% and 5% for the unweighted and weighted regressions, respectively.

There are large differences in mean levels of economic development and air pollution across continents, as is visible from the differentiated concentration of countries from each continent

along the x-axis and y-axis in Figure 8. Specifically, Africa and Asia populate all the quadrants of the figure. In contrast, Europe, the Americas, and Oceania are concentrated in the lower quadrants with dispersion in economic activities but limited variations in air pollution. We analyze the extent to which the air pollution by aerosol and GDP per capita association just documented is explained by the association in continental-level means. We accomplish this in columns (3) and (6) of Panel (a) by introducing continental-level fixed effects to the weighted national and subnational regressions from columns (2) and (5). Globally, we continue to find that higher GDP per capita is associated with less aerosol exposures, but the relationship is significantly weakened—the national-level slope estimate is -0.037 (0.024) and the subnational-level slope estimate is -0.009 (0.009). This result indicates that continental-level mean correlations explain most of the global aerosol and GDP correlation.

Continent-specific Associations In this section, we allow for heterogeneous associations between air pollution by aerosols and GDP per capita in each continent. The previous section assumed that this association is homogeneous across all countries, but depending on the predominant stage that countries in a continent are undergoing, the relationship between air pollution and economic development might differ. In Panel (b) of Table 1, we present estimates for continent-specific associations by allowing for both continent-specific fixed effects as well as continent-specific slopes.

Focusing on the national and subnational population-weighted results in columns (2) and (5) in Panel (b), we find significant variations in the magnitudes of aerosol and GDP association by continents. We find positive slopes for Africa with estimates of 0.023 (s.e. 0.054) and 0.052 (s.e. 0.020) using national and subnational data. The subnational estimate shows that a doubling of GDP per capita for a subnational unit in Africa is associated with a 5.2 percentage points increase in the percentage deviation between the subnational AOD value the the global mean. In contrast, we find significant negative associations in Europe, the Americas, and Oceania, with slopes estimates of -0.016 (s.e. 0.006), -0.019 (s.e. 0.005), and -0.071 (s.e. 0.006) from the subnational results. These indicate that in these areas, higher levels of economic development is associated with lower levels of air pollution by aerosol. Our results for Asia is statistically insignificant, indicating a lack of relationship between economic development and air pollution at the continental level across Asia. We present continent-specific scatter plots using national and subnational data in Appendix Figure C.5.

In columns (3) and (6) of Panel (b), we continue to analyze continent-specific correlations after adding in sub-continental regional group fixed effects. We previously documented significant heterogeneities in sub-continental regional air pollution by aerosol distributions, especially in Asia and Africa. Within each continent, regional average associations between economic development and air pollution could reinforce or mask the GDP and aerosol associations across subnational economic units within each region.

Including subcontinental regional fixed effects and focusing on the subnational results from column (6), our results for Africa, the Americas, Oceania, and Asia are in the same direction but stronger compared to results from column (5) without the subcontinental regional fixed effects. Specifically, we find a positive slope estimate of 0.088 (s.e. 0.023) for Africa. For the Americas and Oceania, we find slope estimates of -0.022 (0.008) and -0.077 (s.e. 0.009). For Asia, the insignificant negative association from column (5) is strengthened to a negative slope of -0.099 (s.e. 0.022)—this means that a doubling of GDP per capita for a subnational unit in Asia is associated with a 9.9 percentage points reduction in the percentage deviation between the subnational AOD value the the global mean. The strengthening of the magnitudes of the slope estimates indicates that the association between GDP and aerosols across subcontinental regions and within subcontinental regions tend to be in opposite directions, especially for Asia.

In contrast to the other continents, in Europe, the slope switches signs after including subcontinental regional fixed effects, column (6) reports a positive slope of 0.053 (s.e. 0.008). This means that looking only at within region variations in GDP and aerosols, a doubling of GDP per capita for a subnational unit in Europe is associated with a 5.3 percentage points increase in the percentage deviation between the subnational AOD value the the global mean. The switch in the sign of the slope indicates that in Europe, regions with higher average GDP per capita tend to have lower average levels of air pollution by aerosols, but controlling for regional means, subnational units with higher GDP tend to have higher air pollution.

5 Discussion and Conclusion

In this paper, using data from around 2010—the most recent year around which reliable granular global population, air pollution by aerosol, and GDP per capita data are jointly available—we document the global relative distribution of air pollution by aerosols across and within regions and countries, and we analyze the global and continental associations between air

pollution by aerosol and GDP per capita.

Our focus on population-weighted distribution of air pollution contrasts with much of the focus in the scientific literature on climate change, which focuses largely on the distribution of climatic burden across locations, with relatively little attention to the relative population exposures to climatic burdens across locations (Mehta et al. 2016; Tian et al. 2023). This paper follows recent works that have combined global gridded population with air pollution data (Shaddick et al. 2018; Van Donkelaar et al. 2021; Van Donkelaar et al. 2016), which have generally focused on analyzing variabilities in regional and national means as well as aggregate distributions for large supra-national groupings. In contrast, our population weighted analysis decomposes the overall global population-weighted air pollution by aerosol distribution into both cross and within region and country components.

The results suggest the existence of pollution inequalities across locations over the globe, with Asian population facing the highest average exposure, followed by populations in Africa, Europe, the Americas, and Oceania. At the continental extremes, Asia's global shares of air pollution by aerosols is 26% larger than its population share, but Oceania's is 63% smaller. We find that the Americas, Europe, and Oceania have distributions with relatively limited variabilities. Europe is the most equal continent in the world with population at the 80^{th} percentile of air pollution by aerosol exposure only 28% more exposed than those at the 20^{th} percentile. In contrast, in Africa and Asia, populations at the 80^{th} percentile of the air pollution by aerosol distribution are 141% and 109% more exposed than population at the 20^{th} percentile, respectively. Across subcontinental regions, the percentage increases in exposure between the 80^{th} and 20^{th} percentiles range from 2% to 208%. This range widens further to from 0% to 359% when we condition further on within country air pollution by aerosol distributions.

The paper also provides evidence about the relationship between pollution burden and economic activity measured by GDP per capita. Overall, we find a strong negative global correlation. In particular, using subnational population-weighted data, we find that a doubling of GDP per capita is associated with a 11.8 percentage points reduction in the percentage deviation between the a subnational unit's population-weighted air pollution by aerosol level and the global population-weighted mean. The association is significantly weakened when continental fixed effects are included, which means the global association is largely explained by correlation between continental-level mean GDP per capita and air pollution by aerosol.

Furthermore, we analyze the GDP and air pollution relationship within each continent.

Exploiting variabilities in subnational data and controlling for aggregate regional variabilities through subcontinental regional fixed effects, we find a positive association between air pollution by aerosols and GDP per capita in Africa and Europe, but negative association in the Americas, Asia, and Oceania. Specifically, we find the strongest negative association in Asia and the strongest positive association in Africa—a doubling of GDP per capita for a subnational unit in Asia and Europe are associated with a 9.9 percentage points reduction and 8.8 percentage points increase in the percentage deviation between the a subnational unit's population-weighted air pollution by aerosol level and the global population-weighted mean, respectively.

There are limitations to our analysis. First, our analysis is centered around one year. While it would be of great interest to compare changes over time, the population census and register data we rely on are from different years centered around 2010 (CIESIN Columbia University 2018), and the subnational GDP dataset we use only has data up to 2010 (Gennaioli et al. 2013) and requires extrapolation to extend the dataset to later years (Kummu, Taka, and Guillaume 2018). Second there are trade-offs between the granularity of cells at which we merge population and air pollution by aerosol data and the precision and availability of cell-specific averages. We use $1^\circ \times 1^\circ$ longitude–latitude grid, which reduces the precision of our population-weighted air pollution by aerosol estimates for smaller countries, but improves the number of raw satellite-based measurements we can draw on to measure air pollution by aerosol exposures for each cell. Third, rather than using climate models to transform AOD to particulate matter measurements (Hammer et al. 2020), for transparency and to reduce the number of intermediating estimation and approximation layers between raw satellite data measurements and inputs for empirical analysis, we use AOD-based measures directly to assess the global distribution of air pollution by aerosols. We present results in AOD levels and in units of relative global excess aerosol burdens. Given the importance of particulate matter to human health, we also provide approximately translated $PM_{2.5}$ values to facilitate the interpretation of our AOD-based results.

References

Bibi, Humera, Khan Alam, Farrukh Chishtie, Samina Bibi, Imran Shahid, and Thomas Blaschke. 2015. "Intercomparison of MODIS, MISR, OMI, and CALIPSO Aerosol Optical Depth Retrievals for Four Locations on the Indo-Gangetic Plains and Validation Against AERONET Data." *Atmospheric Environment* 111 (June 1, 2015): 113–126. https://doi.org/10.1016/j.atmosenv.2015.04.013.

Brabhukumr, Ajith, Prabhjot Malhi, Khaiwal Ravindra, and PVM Lakshmi. 2020. "Exposure to Household Air Pollution During First 3 Years of Life and Iq Level Among 6–8-Year-Old Children in India–a Cross-Sectional Study." *Science of The Total Environment* 709:135110.

Bright, Jamie M., and Christian A. Gueymard. 2019. "Climate-Specific and Global Validation of MODIS Aqua and Terra Aerosol Optical Depth at 452 AERONET Stations." *Solar Energy* 183 (May 1, 2019): 594–605. https://doi.org/10.1016/j.solener.2019.03.043.

Chen, Youliang, Dan Li, Hamed Karimian, Shiteng Wang, and Shuwei Fang. 2022. "The Relationship Between Air Quality and MODIS Aerosol Optical Depth in Major Cities of the Yangtze River Delta." *Chemosphere* 308 (Pt 2): 136301. https://doi.org/10.1016/j.chemosphere.2022.136301.

Chu, Yuanyuan, Yisi Liu, Xiangyu Li, Zhiyong Liu, Hanson Lu, Yuanan Lu, Zongfu Mao, et al. 2016. "A Review on Predicting Ground PM2.5 Concentration Using Satellite Aerosol Optical Depth." *Atmosphere* 7, no. 10 (October): 129. https://doi.org/10.3390/atmos7100129.

CIESIN Columbia University. 2018. *Gridded Population of the World, Version 4 (GPWv4): Basic Demographic Characteristics, Revision 11.* Palisades, New York. https://doi.org/10.7927/H46M34XX.

Cornillon, P., J. Gallagher, and T. Sgouros. 2003. "OPeNDAP: Accessing Data in a Distributed, Heterogeneous Environment." *Data Science Journal* 2:164–174. https://doi.org/10.2481/dsj.2.164.

Fisher, Samantha, David C Bellinger, Maureen L Cropper, Pushpam Kumar, Agnes Binagwaho, Juliette Biao Koudenoukpo, Yongjoon Park, et al. 2021. "Air Pollution and Development in Africa: Impacts on Health, the Economy, and Human Capital." *The Lancet Planetary Health* 5 (10): e681–e688.

Fu, Disong, Xiangao Xia, Jun Wang, Xiaoling Zhang, Xiaojing Li, and Jianzhong Liu. 2018. "Synergy of AERONET and MODIS AOD Products in the Estimation of PM2.5 Concentrations in Beijing." *Scientific Reports* 8, no. 1 (July 5, 2018): 10174. https://doi.org/10.1038/s41598-018-28535-2.

Fu, Shihe, V Brian Viard, and Peng Zhang. 2021. "Air Pollution and Manufacturing Firm Productivity: Nationwide Estimates for China." *The Economic Journal* 131 (640): 3241–3273.

Gakidou, Emmanuela, Ashkan Afshin, Amanuel Alemu Abajobir, Kalkidan Hassen Abate, Cristiana Abbafati, Kaja M Abbas, Foad Abd-Allah, et al. 2017. "Global, Regional, and National Comparative Risk Assessment of 84 Behavioural, Environmental and Occupational, and Metabolic Risks or Clusters of Risks, 1990–2016: A Systematic Analysis for the Global Burden of Disease Study 2016." *The Lancet* 390 (10100): 1345–1422.

Gennaioli, Nicola, Rafael La Porta, Florencio Lopez-de-Silanes, and Andrei Shleifer. 2013. "Human Capital and Regional Development." *The Quarterly Journal of Economics* 128, no. 1 (February 1, 2013): 105–164. https://doi.org/10.1093/qje/qjs050.

Hammer, Melanie S, Aaron van Donkelaar, Chi Li, Alexei Lyapustin, Andrew M Sayer, N Christina Hsu, Robert C Levy, et al. 2020. "Global Estimates and Long-Term Trends of Fine Particulate Matter Concentrations (1998–2018)." *Environmental Science & Technology* 54 (13): 7879–7890.

Holben, B. N., T. F. Eck, I. Slutsker, D. Tanré, J. P. Buis, A. Setzer, E. Vermote, et al. 1998. "AERONET—A Federated Instrument Network and Data Archive for Aerosol Characterization." *Remote Sensing of Environment* 66, no. 1 (October 1, 1998): 1–16. https://doi.org/10.1016/S0034-4257(98)00031-5.

Jacobson, Mark Z. 2002. *Atmospheric Pollution: History, Science, and Regulation.* Cambridge: Cambridge University Press. https://doi.org/10.1017/CBO9780511802287.

Kummu, Matti, Maija Taka, and Joseph HA Guillaume. 2018. "Gridded Global Datasets for Gross Domestic Product and Human Development Index Over 1990–2015." *Scientific data* 5 (1): 1–15.

Lenoble, Jacqueline, Lorraine Remer, and Didier Tanre. 2013. *Aerosol Remote Sensing*. Springer Science & Business Media, February 11, 2013.

Mehta, Manu, Ritu Singh, Ankit Singh, Narendra Singh, and Anshumali. 2016. "Recent Global Aerosol Optical Depth Variations and Trends — a Comparative Study Using MODIS and MISR Level 3 Datasets." *Remote Sensing of Environment* 181 (August 1, 2016): 137–150. https://doi.org/10.1016/j.rse.2016.04.004.

NASA Earth Observatory. 2024. "Aerosol Optical Depth." Aerosol Optical Depth. https://earthobservatory.nasa.gov/global-maps/MODAL2_M_AER_OD.

Odo, Daniel B, Ian A Yang, Sagnik Dey, Melanie S Hammer, Aaron van Donkelaar, Randall V Martin, Guang-Hui Dong, et al. 2023. "A Cross-Sectional Analysis of Long-Term Exposure to Ambient Air Pollution and Cognitive Development in Children Aged 3–4 Years Living in 12 Low-and Middle-Income Countries." *Environmental Pollution* 318:120916.

Pirlea, Florina, and Wendy Ven-dee Huang. 2019. "The Global Distribution of Air Pollution," September 12, 2019. https://datatopics.worldbank.org/world-development-indicators/stories/the-global-distribution-of-air-pollution.html.

Shaddick, Gavin, Matthew L Thomas, Heresh Amini, David Broday, Aaron Cohen, Joseph Frostad, Amelia Green, et al. 2018. "Data Integration for the Assessment of Population Exposure to Ambient Air Pollution for Global Burden of Disease Assessment." *Environmental science & technology* 52 (16): 9069–9078.

Shaddick, Gavin, Matthew L Thomas, Pierpaolo Mudu, Giulia Ruggeri, and Sophie Gumy. 2020. "Half the World's Population Are Exposed to Increasing Air Pollution." *NPJ Climate and Atmospheric Science* 3 (1): 23.

Tian, Xiaomin, Chaoli Tang, Xin Wu, Jie Yang, Fengmei Zhao, and Dong Liu. 2023. "The Global Spatial-Temporal Distribution and EOF Analysis of AOD Based on MODIS Data During 2003–2021." *Atmospheric Environment* 302 (June 1, 2023): 119722. https://doi.org/10.1016/j.atmosenv.2023.119722.

Van Donkelaar, Aaron, Melanie S Hammer, Liam Bindle, Michael Brauer, Jeffery R Brook, Michael J Garay, N Christina Hsu, et al. 2021. "Monthly Global Estimates of Fine Particulate Matter and Their Uncertainty." *Environmental Science & Technology* 55 (22): 15287–15300.

Van Donkelaar, Aaron, Randall V Martin, Michael Brauer, N Christina Hsu, Ralph A Kahn, Robert C Levy, Alexei Lyapustin, et al. 2016. "Global Estimates of Fine Particulate Matter Using a Combined Geophysical-Statistical Method with Information from Satellites, Models, and Monitors." *Environmental science & technology* 50 (7): 3762–3772.

Wang, Qingxin, Dongsheng Du, Siwei Li, Jie Yang, Hao Lin, and Juan Du. 2021. "Comparison of Different Methods of Determining Land Surface Reflectance for AOD Retrieval." *Atmospheric Pollution Research* 12, no. 8 (August 1, 2021): 101143. https://doi.org/10.1016/j.apr.2021.101143.

Xiong, Xiaoxiong, Emily J. Aldoretta, Amit Angal, Tiejun Chang, Xu Geng, Daniel O. Link, Vincent V. Salomonson, et al. 2020. "Terra MODIS: 20 Years of on-Orbit Calibration and Performance." *Journal of Applied Remote Sensing* 14, no. 3 (August): 037501. https://doi.org/10.1117/1.JRS.14.037501.

Yang, Qianqian, Qiangqiang Yuan, Linwei Yue, Tongwen Li, Huanfeng Shen, and Liangpei Zhang. 2019. "The Relationships Between PM2.5 and Aerosol Optical Depth (AOD) in Mainland China: About and Behind the Spatio-Temporal Variations." *Environmental Pollution* 248 (May 1, 2019): 526–535. https://doi.org/10.1016/j.envpol.2019.02.071.

Figure 1: Global population-weighted distribution of air pollution by aerosols, 2010

(a) Country as the unit of observation (weighted by country-population)

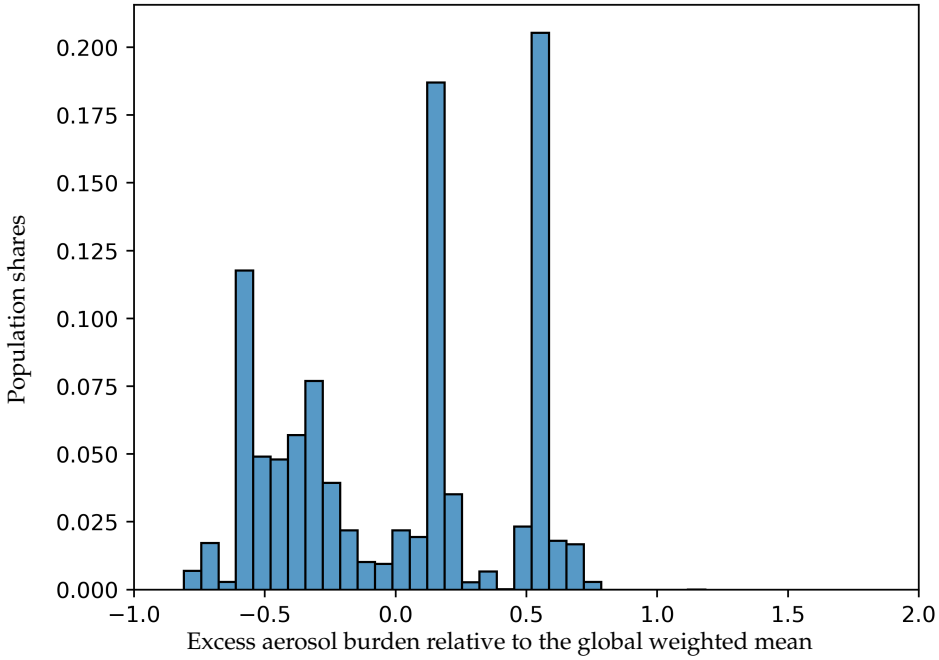

(b) 1° cell as the unit of observation (weighted by cell-population)

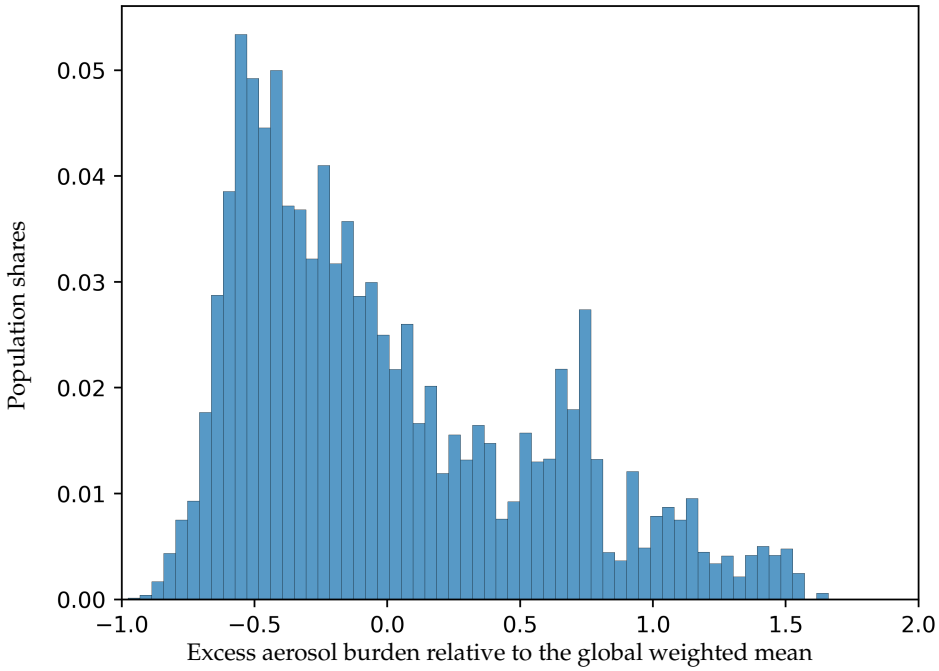

Notes: The panels present the global relative distribution of air pollution by aerosols as measured by Aerosol Optical Depth (AOD). We compute annual average AOD for each cell ($1° \times 1°$ longitude–latitude grid) and then generate country-specific AOD as cell-population weighted averages. The country-based distribution in Panel (a) uses country-specific AOD, weighted by aggregate population estimates for each country. The cell-based distribution in Panel (b) uses cell-specific AOD, weighted by cell-specific population estimates. The x-axes are in units of what we call global excess aerosol burden: A value of 0.5 (-0.5) indicates that a country or cell's AOD measure is 50 percent greater (smaller) than the global weighted mean.

Figure 2: Continental population-weighted distribution of air pollution by aerosols, 2010

(a) 1° cell (1° × 1° longitude–latitude grid) as the unit of observation map

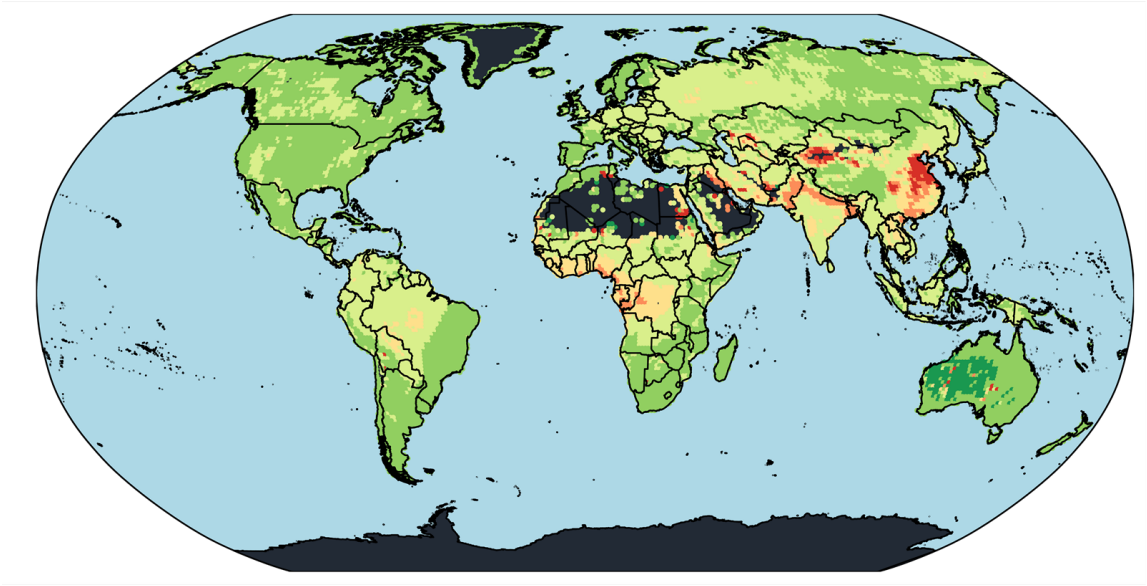

(b) 1° cell as the unit of observation (weighted by cell-population), by regions

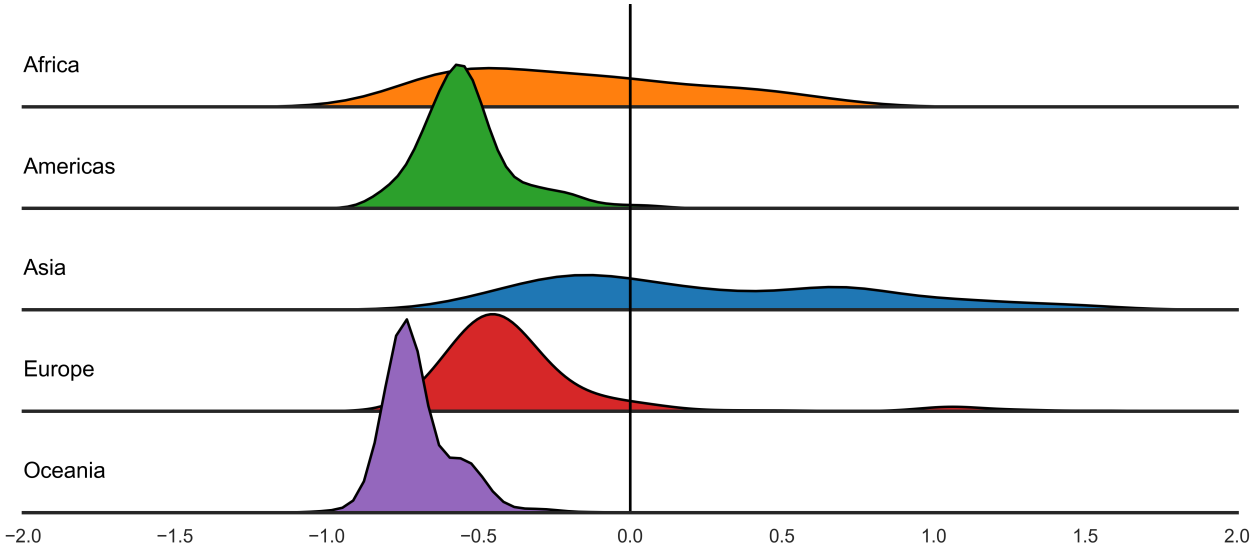

Notes: The panels present the global relative distribution of air pollution by aerosols as measured by Aerosol Optical Depth (AOD). We compute annual average AOD for each 1° cell. The map in Panel (a) matches cell-specific AOD to cell locations. The distribution in Panel (b) uses cell-specific AOD, weighted by cell-specific population estimates. The y-axis in Panel (b) shows cell population weighted density approximations. The colors in Panel (a) and x-axis in Panel (b) correspond to what we call global excess aerosol burden: A value of 0.5 (-0.5) indicates that a cell's AOD measure is 50 percent greater (smaller) than the global weighted mean. In Panel (b), darker shades of green (red) correspond to greater magnitudes of negative (positive) excess burdens.

Figure 3: African population-weighted distribution of air pollution by aerosols, 2010

(a) 1° cell as the unit of observation (weighted by cell-population), by sub-regions

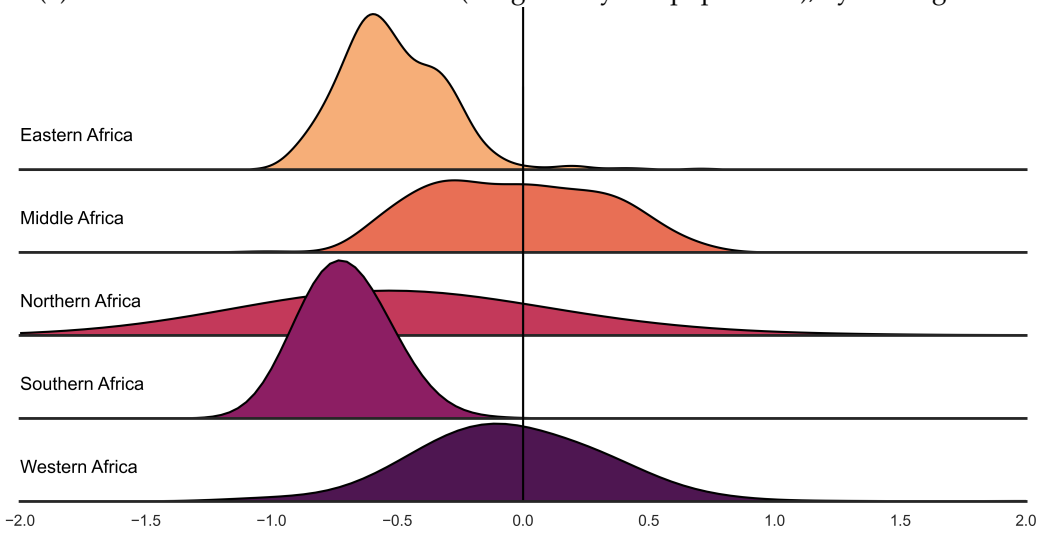

(b) Country-specific distributional ranges: P20 (*left-dot*), mean (*center-dot*), P80 (*right-dot*)

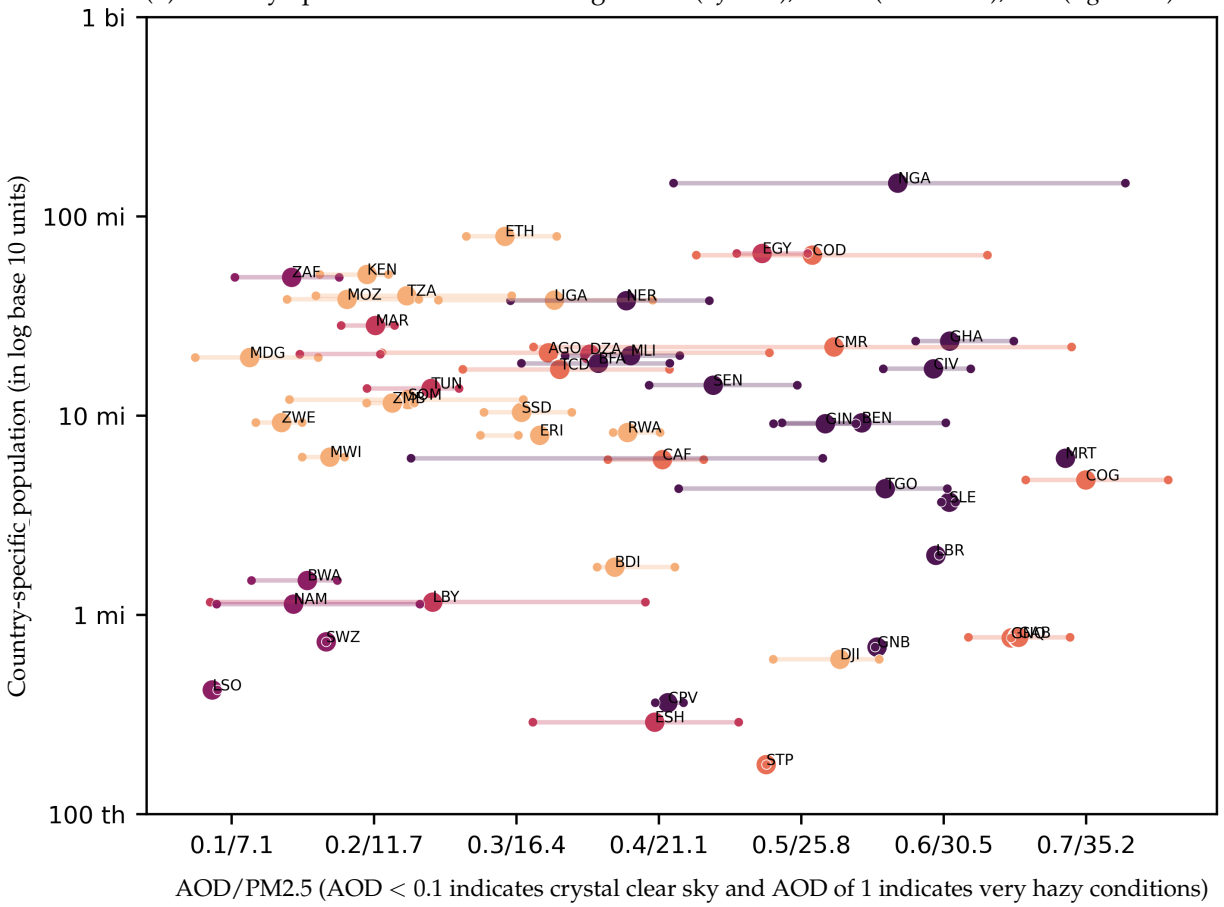

Notes: The panels present the African distribution of air pollution by aerosols as measured by Aerosol Optical Depth (AOD). We compute annual average AOD for each 1° cell. Panel (b) lines mark the 20th percentile, mean, and the 80th percentile of a country's AOD distribution, computed based on the distribution of AOD and population across cells corresponding to each country. In Panel (a), the y-axis shows cell population weighted density approximations. The x-axis in Panel (a) corresponds to levels of excess aerosol burden, a value of 0.5 (-0.5) indicates that a cell's AOD measure is 50 percent greater (smaller) than the global weighted mean. The x-axis in Panel (b) is in AOD units, and the tick-labels show AOD values and corresponding PM 2.5 estimates in $\mu g/m^3$ units, separated by backslash.

Figure 4: American population-weighted distribution of air pollution by aerosols, 2010

(a) 1° cell as the unit of observation (weighted by cell-population), by sub-regions

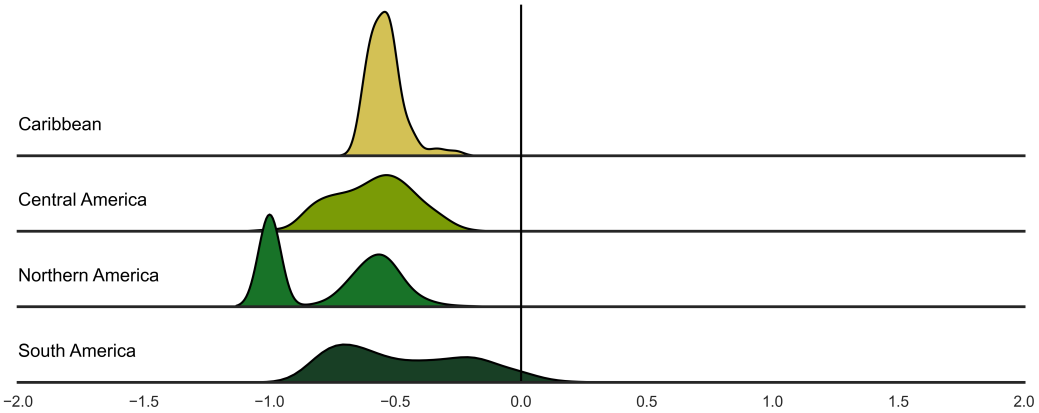

Excess aerosol burden relative to the global weighted mean

(b) Country-specific distributional ranges: P20 (*left-dot*), mean (*center-dot*), P80 (*right-dot*)

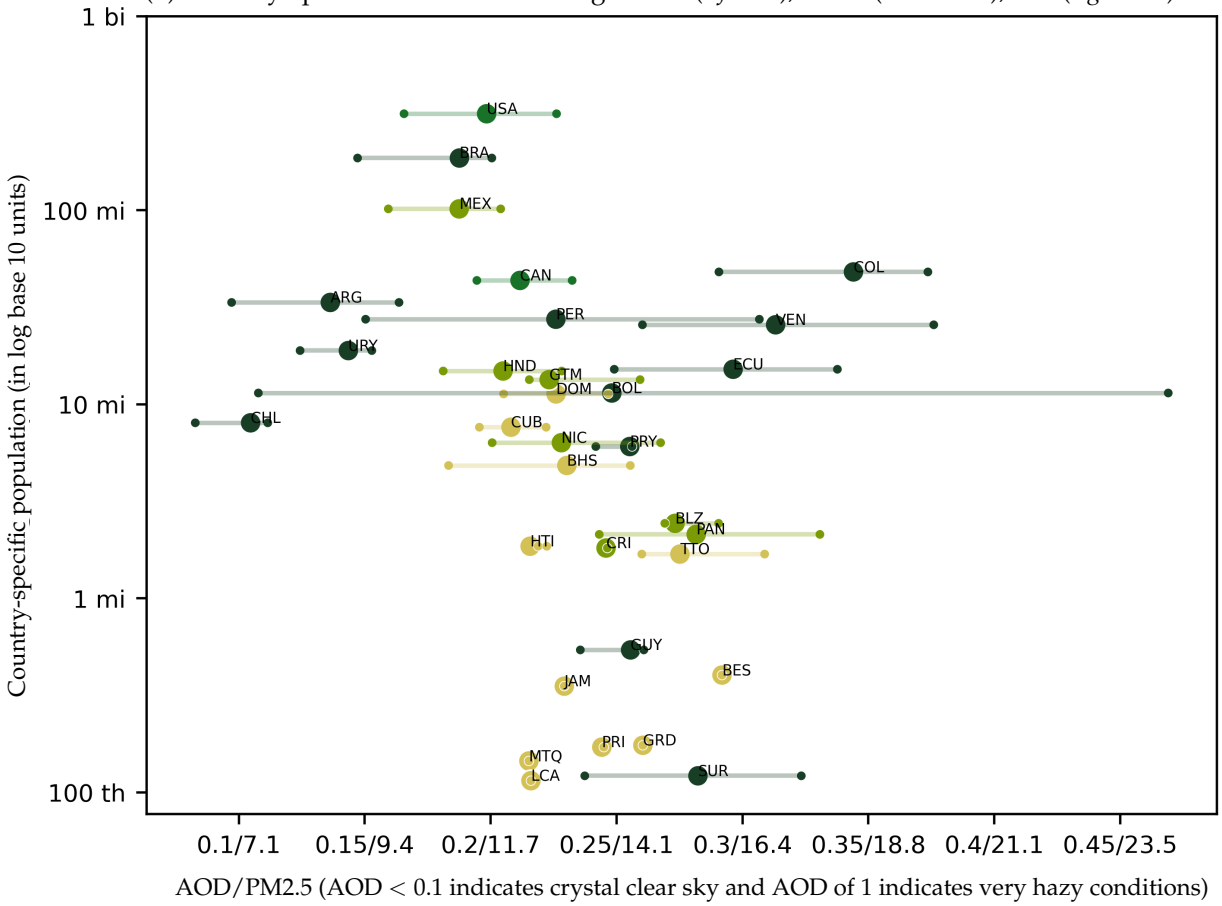

AOD/PM2.5 (AOD < 0.1 indicates crystal clear sky and AOD of 1 indicates very hazy conditions)

Notes: The panels present the American distribution of air pollution by aerosols as measured by Aerosol Optical Depth (AOD). We compute annual average AOD for each 1° cell. Panel (b) lines mark the 20th percentile, mean, and the 80th percentile of a country's AOD distribution, computed based on the distribution of AOD and population across cells corresponding to each country. In Panel (a), the y-axis shows cell population weighted density approximations. The x-axis in Panel (a) corresponds to levels of excess aerosol burden, a value of 0.5 (-0.5) indicates that a cell's AOD measure is 50 percent greater (smaller) than the global weighted mean. The x-axis in Panel (b) is in AOD units, and the tick-labels show AOD values and corresponding PM 2.5 estimates in $\mu g/m^3$ units, separated by backslash.

Figure 5: Asian population-weighted distribution of air pollution by aerosols, 2010

(a) 1° cell as the unit of observation (weighted by cell-population), by sub-regions

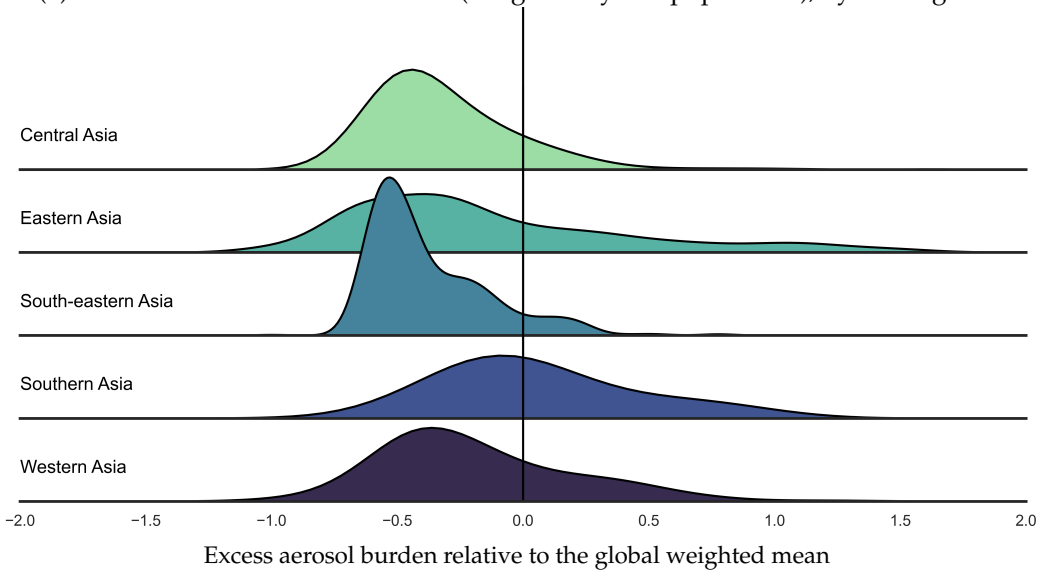

(b) Country-specific distributional ranges: P20 (*left-dot*), mean (*center-dot*), P80 (*right-dot*)

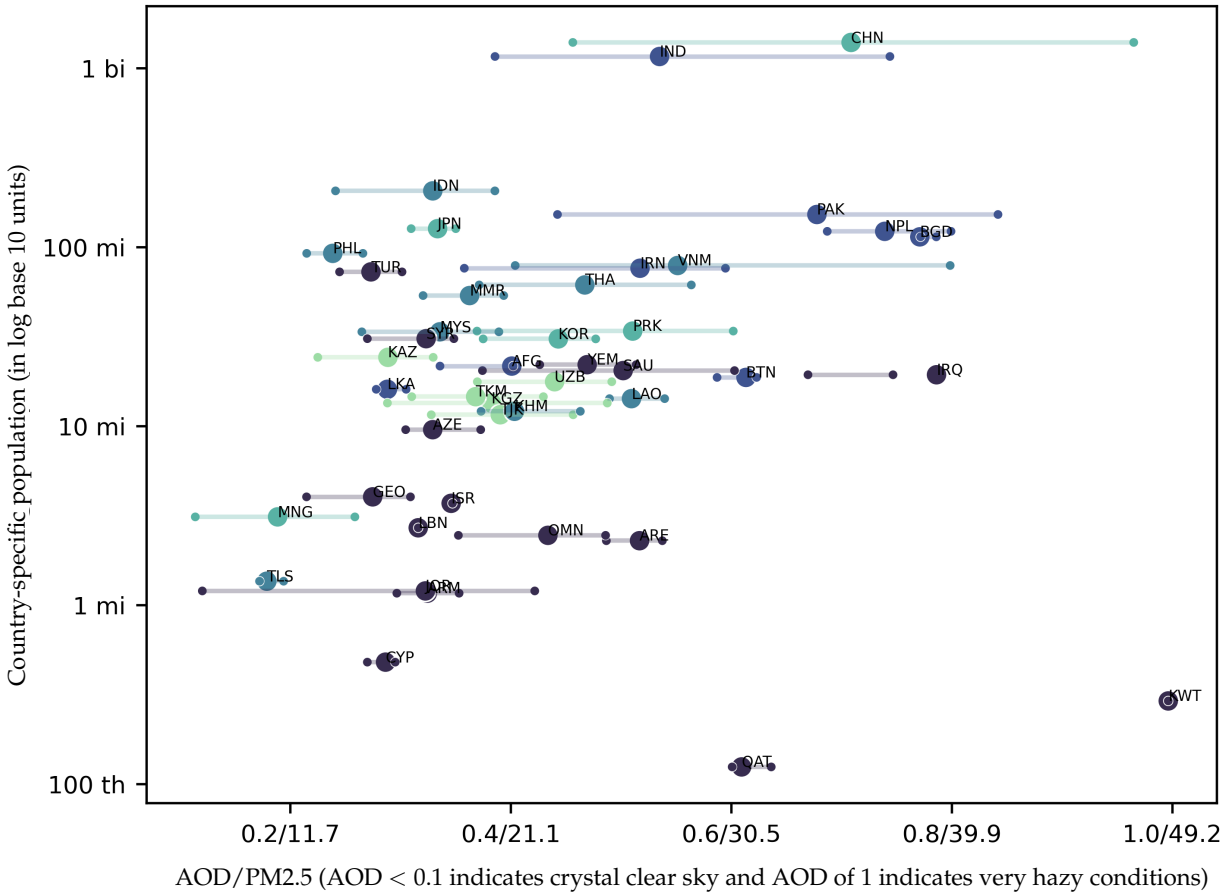

Notes: The panels present the Asian distribution of air pollution by aerosols as measured by Aerosol Optical Depth (AOD). We compute annual average AOD for each 1° cell. Panel (b) lines mark the 20th percentile, mean, and the 80th percentile of a country's AOD distribution, computed based on the distribution of AOD and population across cells corresponding to each country. In Panel (a), the y-axis shows cell population weighted density approximations. The x-axis in Panel (a) corresponds to levels of excess aerosol burden, a value of 0.5 (-0.5) indicates that a cell's AOD measure is 50 percent greater (smaller) than the global weighted mean. The x-axis in Panel (b) is in AOD units, and the tick-labels show AOD values and corresponding PM 2.5 estimates in $\mu g/m^3$ units, separated by backslash.

Figure 6: European population-weighted distribution of air pollution by aerosols, 2010

(a) 1° cell as the unit of observation (weighted by cell-population), by sub-regions

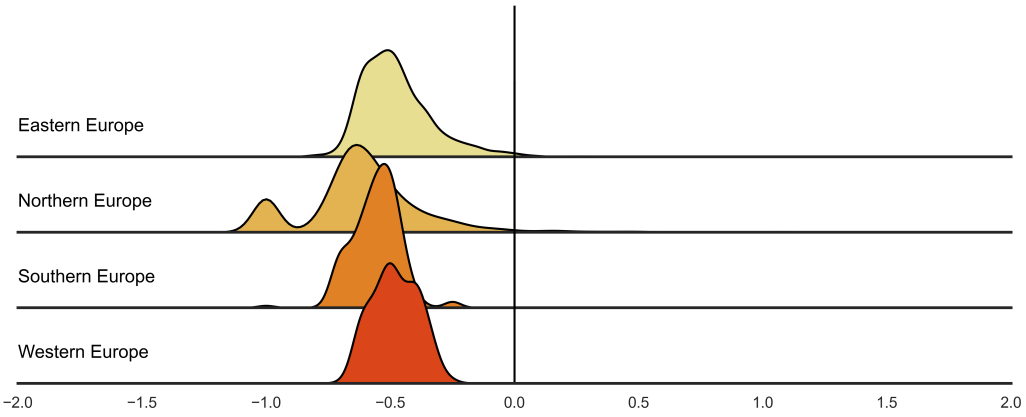

Excess aerosol burden relative to the global weighted mean

(b) Country-specific distributional ranges: P20 (*left-dot*), mean (*center-dot*), P80 (*right-dot*)

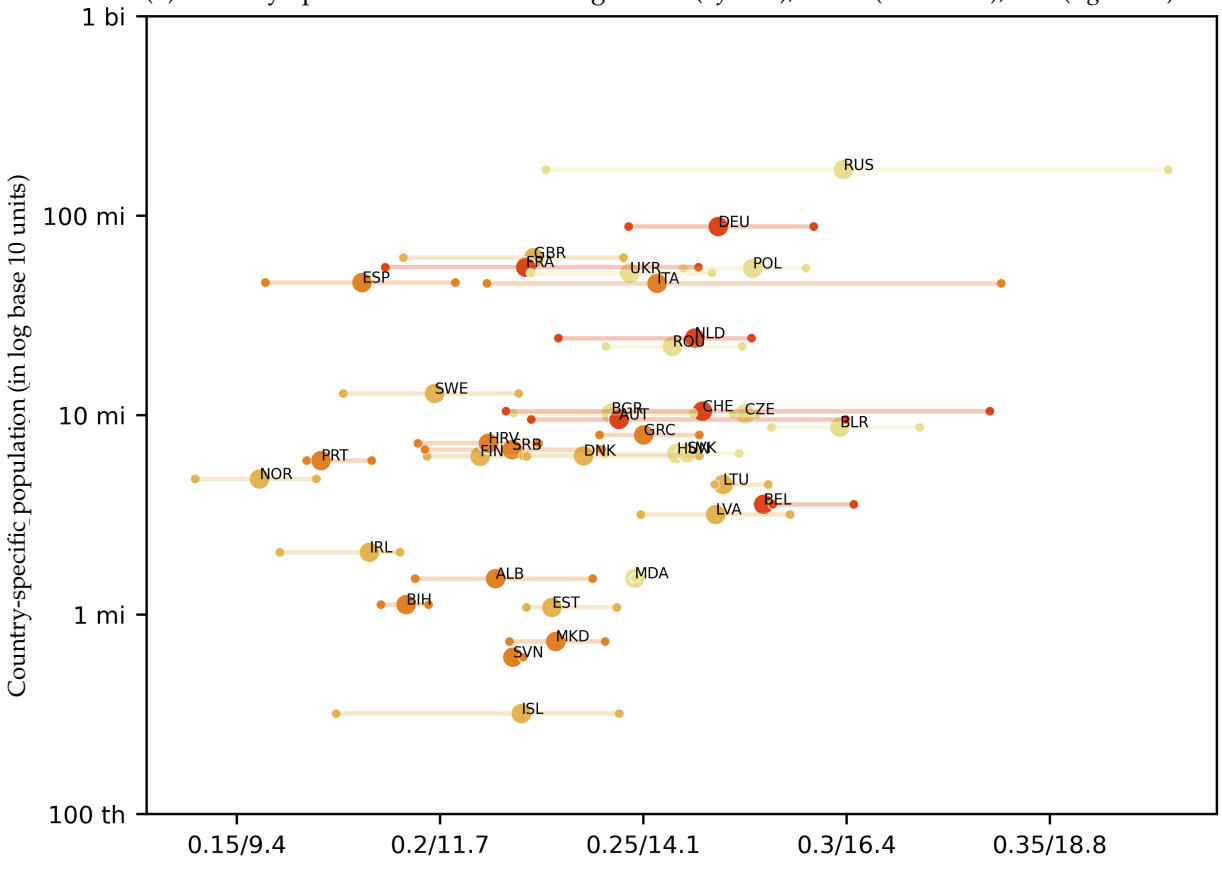

AOD/PM2.5 (AOD $<$ 0.1 indicates crystal clear sky and AOD of 1 indicates very hazy conditions)

Notes: The panels present the European distribution of air pollution by aerosols as measured by Aerosol Optical Depth (AOD). We compute annual average AOD for each 1° cell. Panel (b) lines mark the 20th percentile, mean, and the 80th percentile of a country's AOD distribution, computed based on the distribution of AOD and population across cells corresponding to each country. In Panel (a), the y-axis shows cell population weighted density approximations. The x-axis in Panel (a) corresponds to levels of excess aerosol burden, a value of 0.5 (-0.5) indicates that a cell's AOD measure is 50 percent greater (smaller) than the global weighted mean. The x-axis in Panel (b) is in AOD units, and the tick-labels show AOD values and corresponding PM 2.5 estimates in $\mu g/m^3$ units, separated by backslash.

Figure 7: Oceanian population-weighted distribution of air pollution by aerosols, 2010

(a) 1° cell as the unit of observation (weighted by cell-population), by sub-regions

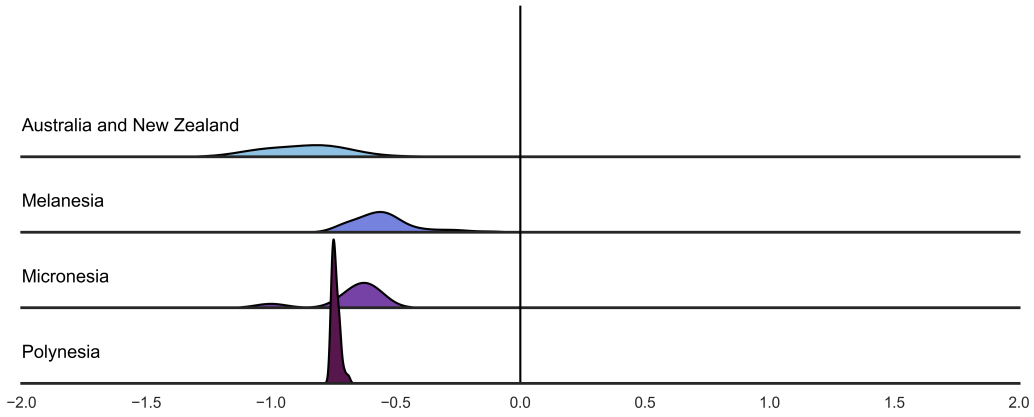

Excess aerosol burden relative to the global weighted mean

(b) Country-specific distributional ranges: P20 (*left-dot*), mean (*center-dot*), P80 (*right-dot*)

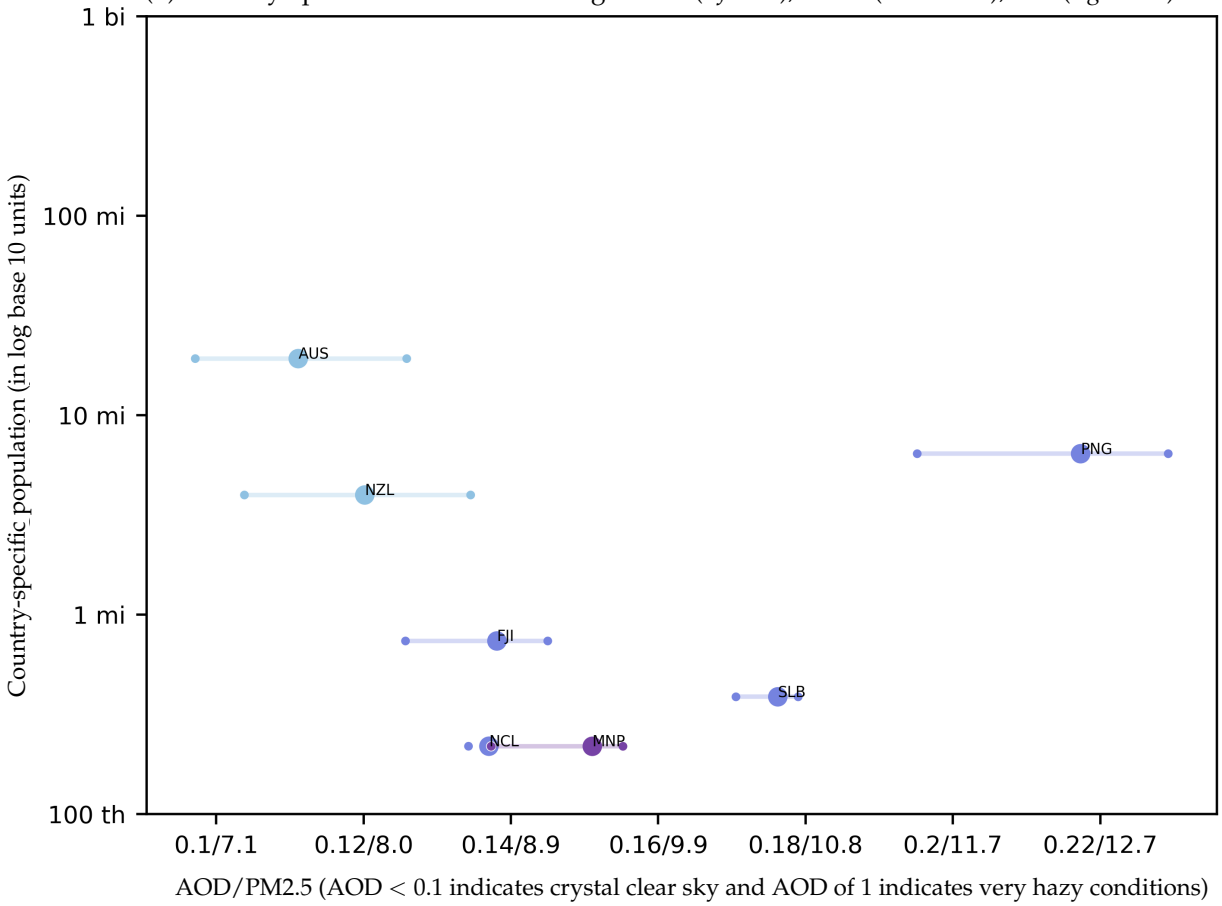

AOD/PM2.5 (AOD < 0.1 indicates crystal clear sky and AOD of 1 indicates very hazy conditions)

Notes: The panels present Oceanian distribution of air pollution by aerosols as measured by Aerosol Optical Depth (AOD). We compute annual average AOD for each 1° cell. Panel (b) lines mark the 20th percentile, mean, and the 80th percentile of a country's AOD distribution, computed based on the distribution of AOD and population across cells corresponding to each country. In Panel (a), the y-axis shows cell population weighted density approximations. The x-axis in Panel (a) corresponds to levels of excess aerosol burden, a value of 0.5 (-0.5) indicates that a cell's AOD measure is 50 percent greater (smaller) than the global weighted mean. The x-axis in Panel (b) is in AOD units, and the tick-labels show AOD values and corresponding PM 2.5 estimates in $\mu g/m^3$ units, separated by backslash.

Figure 8: Global association between air pollution by aerosols and GDP per capita, 2010

(a) National scatter plot, continental color groups, circle size represents relative population sizes

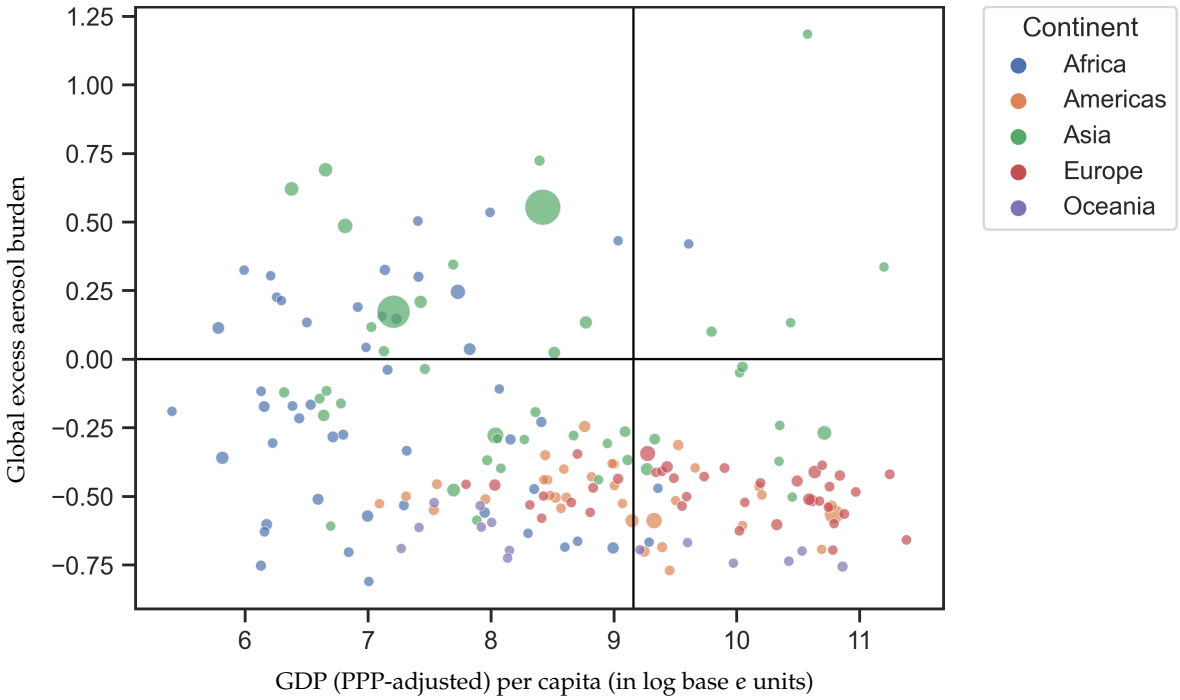

(b) National scatter plot, national population weighted bivariate regression line

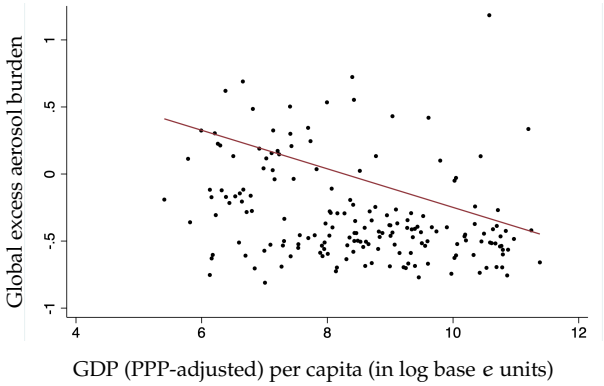

(c) Subnational scatter plot, subnational population weighted bivariate regression line

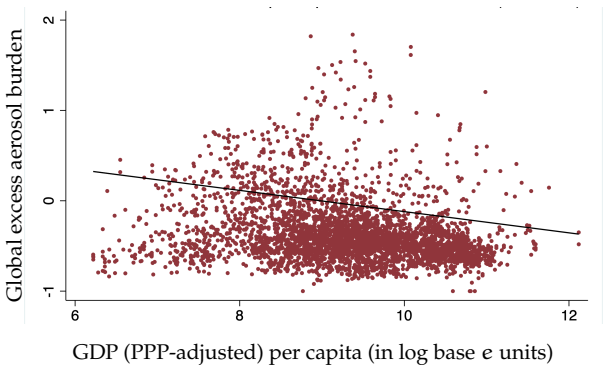

Notes: Panels (a) and (b) present national aggregates. Panel (c) presents subnational—first-level subnational administrative division—results. Across the panels, the x-axes correspond to levels of economic development as measured by GDP (Purchasing Price Parity adjusted) per capita in log base e units, and the y-axes correspond to relative exposures to air pollution by aerosols as measured by Aerosol Optical Depth (AOD). In Panel (a), colors distinguish countries by continental groupings, and the size of the scatter points are proportional to population sizes of each country. Additionally, in Panel (a), the black lines mark global weighted averages along each axis and divide countries into four quadrants for relative comparisons: upper-right, higher GDP per capita and AOD; upper-left, lower GDP per capita and higher AOD; bottom-left, lower GDP per capita and AOD; and bottom-right, higher GDP per capita and lower AOD. The y-axes across panels are in units of what we call global excess aerosol burden: A value of 0.5 (-0.5) indicates that a national or subnational unit's AOD measure is 50 percent greater (smaller) than the global weighted mean. We compute annual average AOD for each cell ($1° \times 1°$ longitude–latitude grid) and then generate national and subnational AOD as cell-population weighted averages. Subnational GDP and boundaries come from Kummu, Taka, and Guillaume (2018).

Table 1: Global association between air pollution by aerosols and GDP per capita, 2010

	Dependent variable: global excess aerosol burden					
	National regressions			Subnational regressions		
	(1)	(2)	(3)	(4)	(5)	(6)
(a): Common-slope global regressions						
GDP (PPP-adjusted) per capita (in log base e units)						
× Global	-0.075***	-0.144***	-0.037	-0.083***	-0.118***	-0.009
	(0.018)	(0.023)	(0.024)	(0.007)	(0.008)	(0.009)
R^2	0.09	0.19	0.57	0.04	0.05	0.37
Observations	178	178	178	3,902	3,712	3,709
Population weights	No	Yes	Yes	No	Yes	Yes
Continental fixed effects	No	No	Yes	No	No	Yes
(b): Continent-specific slope regressions						
GDP (PPP-adjusted) per capita (in log base e units)						
× Africa	-0.031	0.023	0.032	0.099***	0.052**	0.088***
	(0.053)	(0.054)	(0.060)	(0.027)	(0.020)	(0.023)
× Americas	-0.031	-0.027	-0.074*	-0.057***	-0.019***	-0.022***
	(0.021)	(0.018)	(0.041)	(0.011)	(0.005)	(0.008)
× Asia	-0.013	-0.053	-0.253***	-0.030	-0.026	-0.099***
	(0.044)	(0.054)	(0.045)	(0.022)	(0.021)	(0.022)
× Europe	-0.019	-0.037**	0.032	-0.055***	-0.016**	0.053***
	(0.014)	(0.014)	(0.020)	(0.006)	(0.006)	(0.008)
× Oceania	-0.040***	-0.065***	-0.064**	-0.061***	-0.071***	-0.077***
	(0.013)	(0.005)	(0.024)	(0.012)	(0.006)	(0.009)
Observations	178	178	178	3,902	3,712	3,709
Population weights	No	Yes	Yes	No	Yes	Yes
Continental fixed effects	Yes	Yes	Yes	Yes	Yes	Yes
Sub-continental fixed effects	No	No	Yes	No	No	Yes

Note: * $p < 0.1$; ** $p < 0.05$; *** $p < 0.01$. We regress global excess aerosol burden—which captures global relative exposures to air pollution by aerosols as measured by Aerosol Optical Depth (AOD)—on GDP (Purchasing Price Parity adjusted) per capita in log base e units. Results in Panel (a) present the global association, and results in Panel (b) allow for continent-specific associations. In columns (1)–(3), we use country-level data; in columns (4)–(6), we use subnational—first-level subnational administrative division—data. Results from columns (1) and (4) give equal weights to each national and subnational unit. Results from columns (2) and (5) use national or subnational population weights. In Panel (a), results from columns (3) and (6) control for continental fixed effects. In Panel (b), all columns allow for continent-specific slopes and intercepts, and columns (3) and (6) also control for sub-continental fixed effects for each sub-region shown in Panel (a) from Figures 3–6 (e.g., Northern Africa, East Asia, etc.). The dependent variable across regressions is in units of what we call global excess aerosol burden: A value of 0.5 (-0.5) indicates that a national or subnational unit's AOD measure is 50 percent greater (smaller) than the global weighted mean. We compute annual average AOD for each cell ($1^\circ \times 1^\circ$ longitude–latitude grid) and then generate national and subnational AOD as cell-population weighted averages. Subnational GDP and boundaries come from Kummu, Taka, and Guillaume (2018). See Figure 8 and Appendix Figure C.5 for scatter plots corresponding to panels (a) and (b).

ONLINE APPENDIX

Population burdens of air pollution around the world: Distributions, inequalities, and links to per capita GDP

Angelo Santos, Oscar Morales, Jere Behrman, Emily Hannum, Fan Wang

A Program and Framework for analysis

The key file inputs make possible the merge between the geocoded pollution, population, and country datasets. In our analysis, we used two file inputs:

1. k̈ey_loc.csvänd
2. k̈ey_country_code_finer_subregions.csv.

The first key file has an id for every latitude-longitude combination at 1 degree level. The IDs were constructed using the following pattern. The latitude and longitude numbers were transformed into strings and concatenated (using "_" to separate the numbers) into one string called "geo_id ". For example, the location defined by latitude 45 and longitude -67 has the geo_id as "45_-67". After constructing all the possible geo_ids combinations, we sorted the location by latitude and longitude and assigned a number to each geo_id following the ascending order. This new column is called id_location and it is used to merge locations across different datasets, such as the pollution and the population geocoded information.

The second key file has the id_location and geo_id columns associated with geographical locations in the world. four layers of location: continent, subregion, and country. For instance, we know what are the latitude and longitude combinations that are associated with specific continents, sub-regions, and countries, which makes it possible to merge geocoded information from other datasets.

B Additional Figures and Tables

Figure C.1: Number of days with AOD data available at each 1° × 1° longitude–latitude grid, 2010

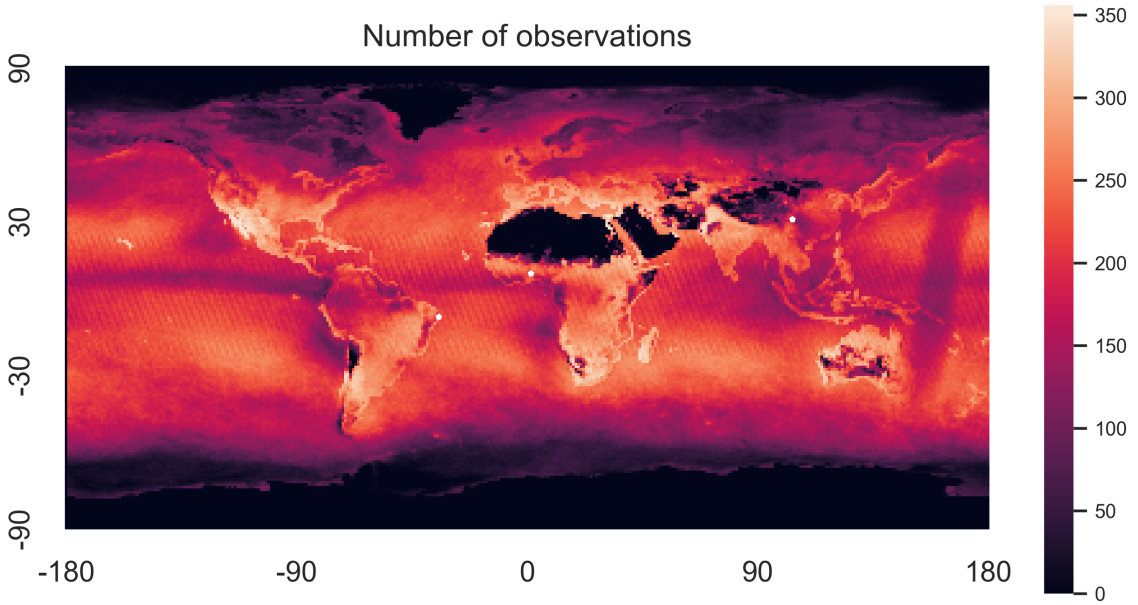

Notes: The figure presents the geographical and temporal availability of Aerosol Optical Depth (AOD) data, our global proxy for ambient particulate matter pollution exposures. For our analysis, we download raw AOD data available at 3km × 3km resolution and compute average daily AOD on each day of the year with available AOD measurements for each 1° × 1° longitude–latitude grid (cell). The figure shows the number of days in 2010 during which AOD data was available within each cell. The days are represented through shades of red from the darkest red (0 days) to the lightest red (all days in the year). On days in which we do not have available AOD information for a particular cell, we use information in neighboring locations and time periods to perform 3-dimensional—longitude, latitude, and time—interpolation and extrapolation to generate estimates for missing AOD data. Given daily information, we compute annual average AOD exposures for each cell, first using only the raw data ignoring the days with missing values, and then separately using the raw data complemented with the interpolated and extrapolated estimates. Due to the concentration of missing AOD data in regions with the least population, our population-weighted AOD distributional results based on the raw data and interpolated and extrapolated data are very similar. Our global inequality results presented in the text are based on annual averages of the raw data.

Figure C.2: Global dispersion of air pollution by aerosols, 2010

(a) Country as the unit of observation (equal weight for each country)

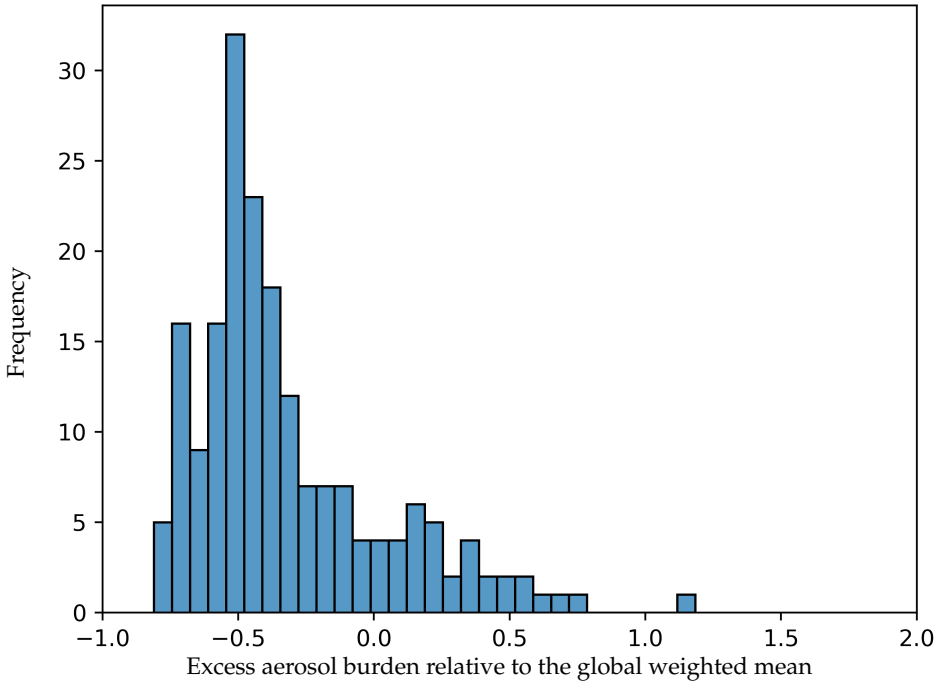

(b) 1° cell as the unit of observation (equal weight for each cell)

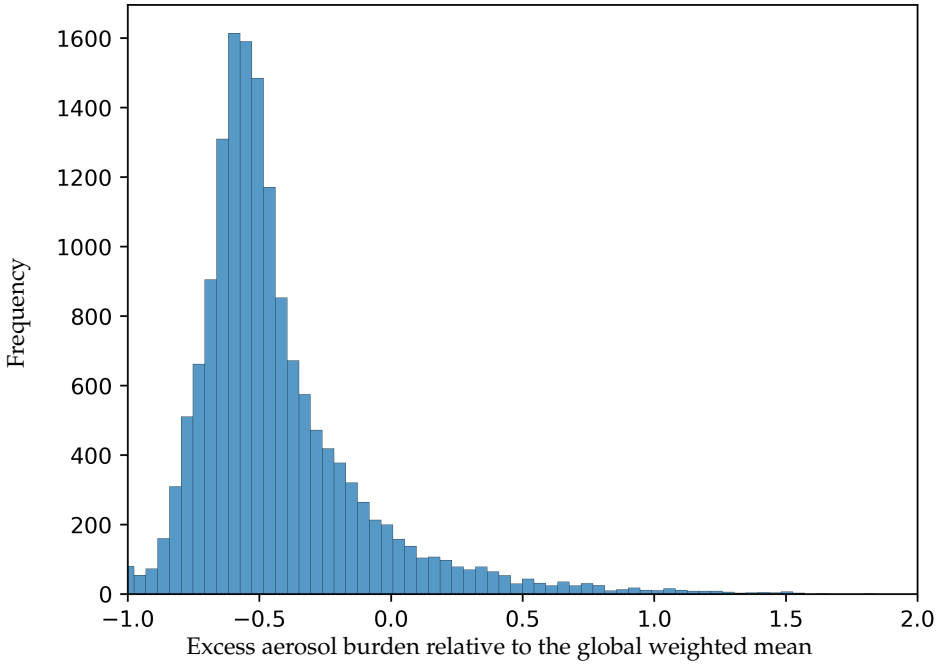

Notes: The panels present the global relative dispersion of air pollution by aerosols as measured by Aerosol Optical Depth (AOD). We compute annual average AOD for each cell ($1° \times 1°$ longitude–latitude grid) and then generate country-specific AOD as cell-population weighted averages. In contrast to Figure 1, Panel (a) and (b) here treat each country or cell as a unit of observation with equal weights. The y-axis shows frequencies, counting the number of countries or cells. The x-axis is in units of what we call global excess aerosol burden: A value of 0.5 (-0.5) indicates that a country or cell's AOD measure is 50 percent greater (smaller) than the global weighted mean.

Figure C.3: Continental dispersion of air pollution by aerosols, 2010

(a) Country as the unit of observation (weighted by country-population), by continents

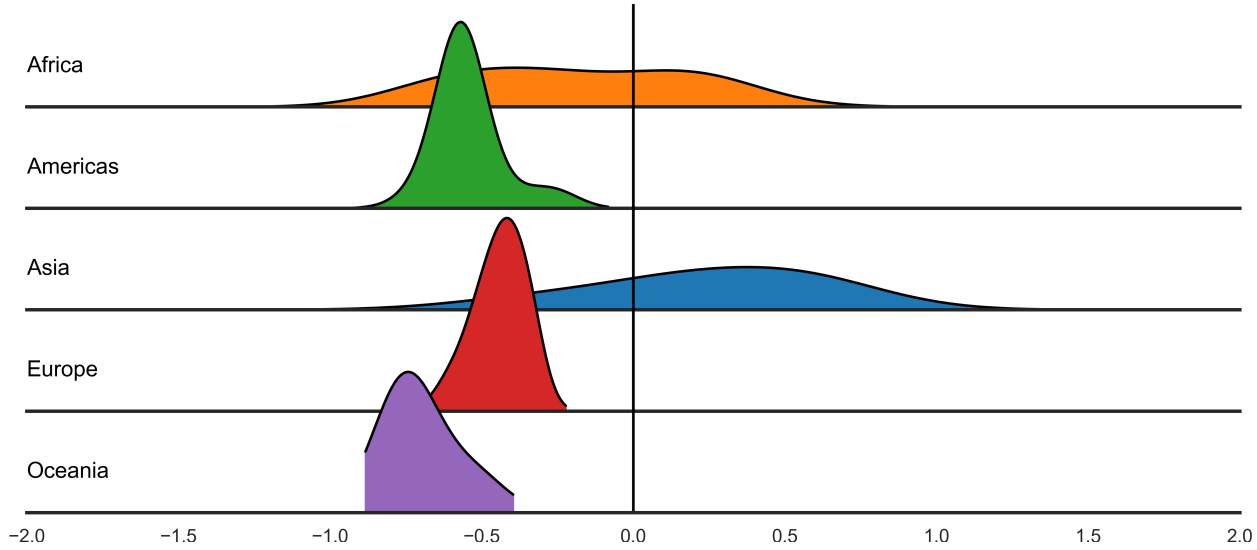

(b) Country as the unit of observation map

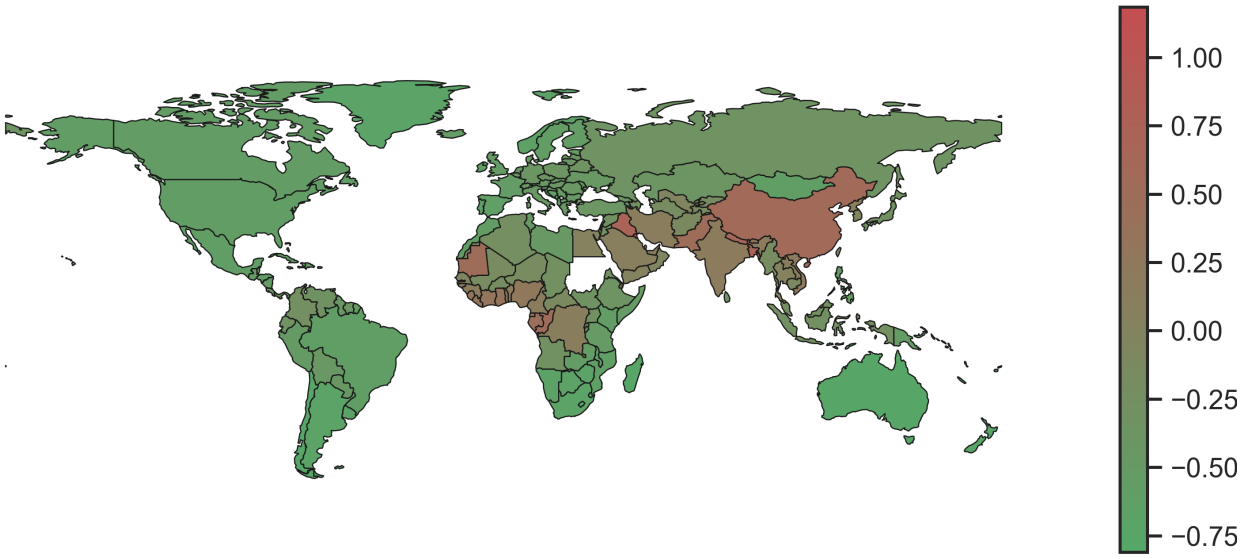

Notes: The panels present the global relative dispersion of air pollution by aerosols as measured by Aerosol Optical Depth (AOD). We compute annual average AOD for each cell ($1° \times 1°$ longitude–latitude grid) and then generate country-specific AOD as cell-population weighted averages. In contrast to Figure 2, Panel (a) treats each country as the unit of observation, weighted by aggregate population estimates for each country, and Panel (b) matches country-specific AOD to country locations. In Panel (a), the y-axis shows country population weighted density approximations. The x-axis in Panel (a) and colors in Panel (b) correspond to what we call global excess aerosol burden: A value of 0.5 (-0.5) indicates that a country's AOD measure is 50 percent greater (smaller) than the global weighted mean. In Panel (b), darker shades of green (red) correspond to greater magnitudes of negative (positive) excess burdens.

Figure C.4: Continental dispersion of air pollution by aerosols, relative to continent-specific weighted means, 2010

(a) Africa

(b) Americas

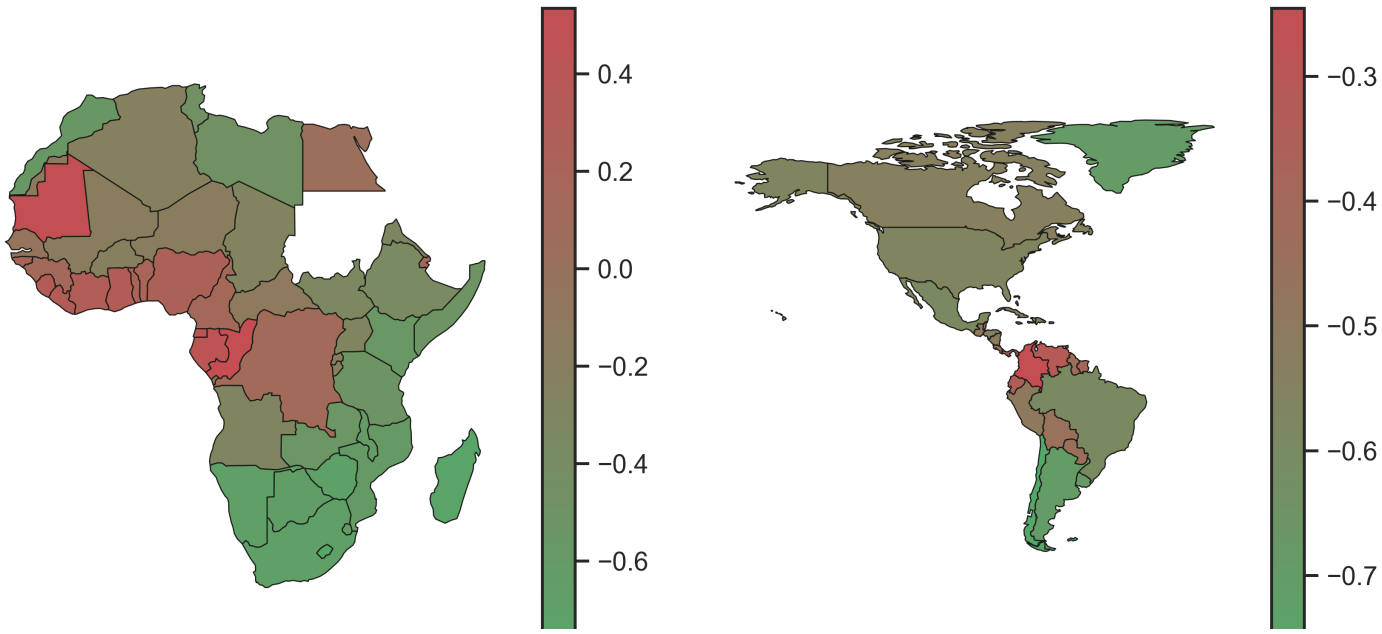

(c) Asia

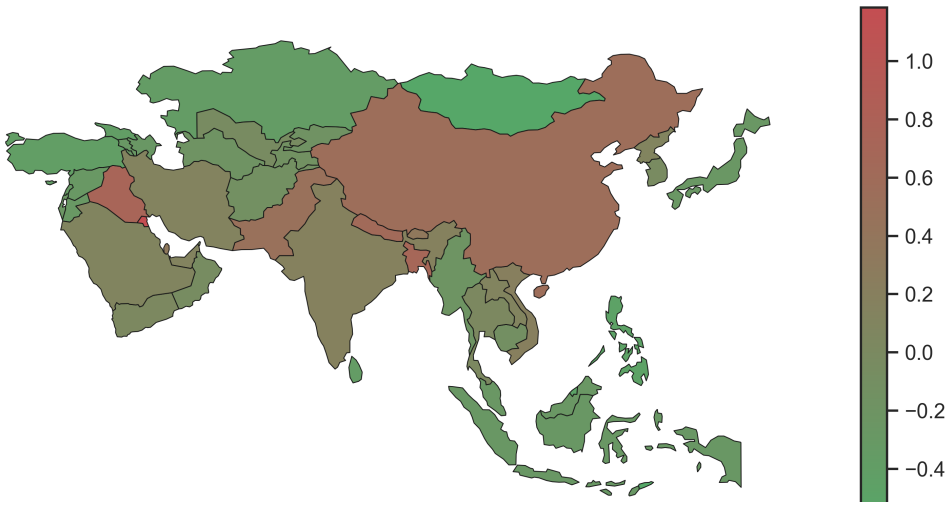

Note: The panels present the continent-specific relative dispersion of air pollution by aerosols as measured by Aerosol Optical Depth (AOD). We compute annual average AOD for each cell ($1° \times 1°$ longitude–latitude grid) and then generate country-specific AOD as cell-population weighted averages. The colors in each Panel correspond to levels of what we call continental excess aerosol burden: A value of 0.5 (-0.5) indicates that a country's AOD measure is 50 percent greater (smaller) than the continental weighted mean. In all Panels, darker shades of green (red) correspond to greater magnitudes of negative (positive) excess burdens.

Figure C.5: Continental association between air pollution by aerosols and GDP per capita, 2010

(a) National scatter plots, national population weighted bivariate regression lines

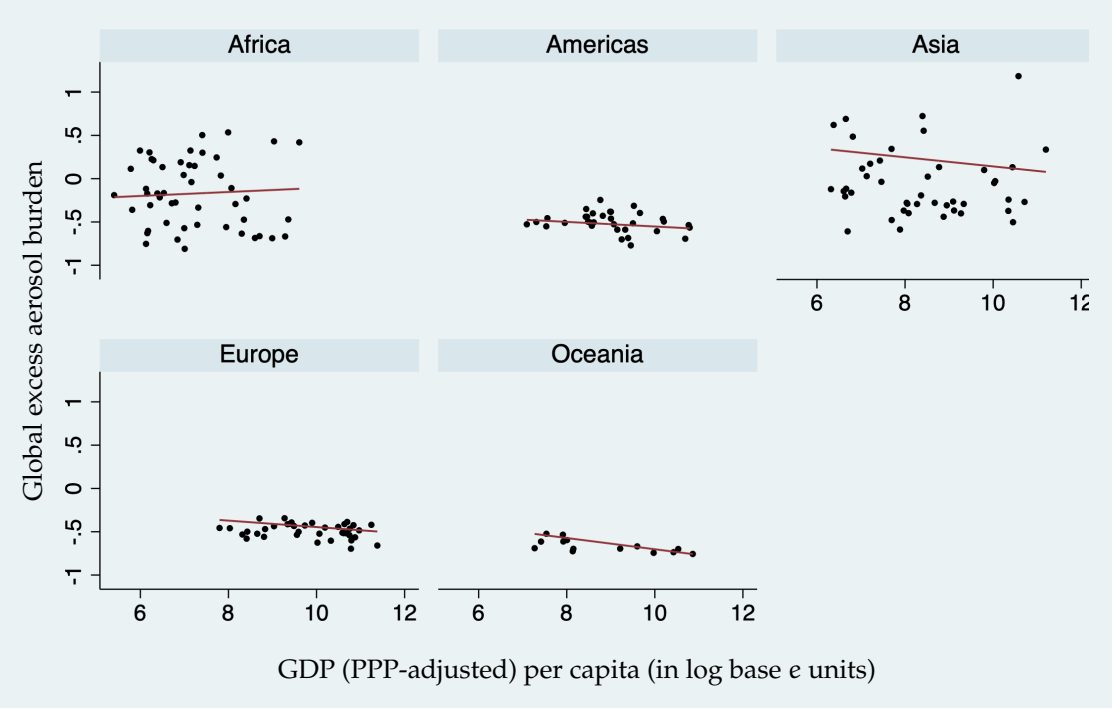

(b) Subnational scatter plots, subnational population weighted bivariate regression lines

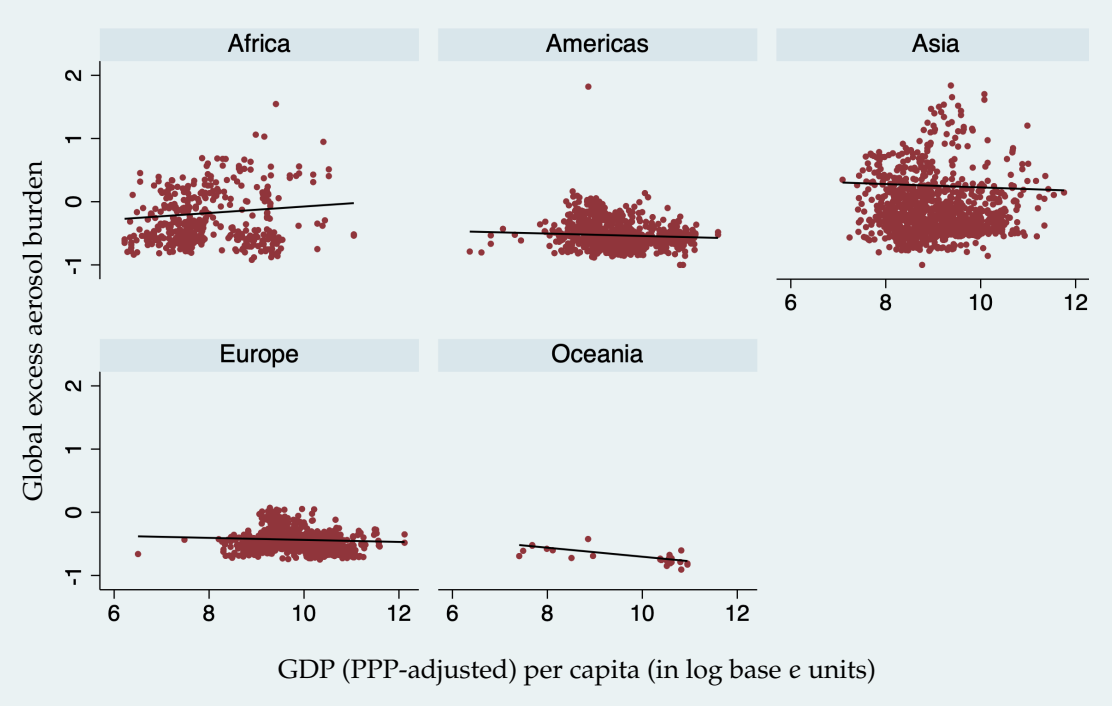

Notes: Across the panels, the x-axes correspond to levels of economic development as measured by GDP (Purchasing Price Parity adjusted) per capita in log base e units, and the y-axes correspond to relative exposures to air pollution by aerosols as measured by Aerosol Optical Depth (AOD). The y-axes across panels are in units of what we call global excess aerosol burden: A value of 0.5 (-0.5) indicates that a national or subnational unit's AOD measure is 50 percent greater (smaller) than the global weighted mean. We compute annual average AOD for each cell ($1° \times 1°$ longitude–latitude grid) and then generate national and subnational AOD as cell-population weighted averages. Subnational GDP and boundaries come from Kummu, Taka, and Guillaume (2018). See Figure 8 for global results and see Table 1 for regression coefficients.

Table C.1: Continental population-weighted distribution of air pollution by aerosols, 2010

	Population weighted means		Within-group AOD distributions	
Continent	AOD	Excess aerosol burden	P80 to P20 ratio	P90 to P10 ratio
Africa	0.37	-0.18	2.78	4.01
Americas	0.21	-0.54	1.56	2.23
Asia	0.57	0.25	2.25	3.18
Europe	0.25	-0.44	1.36	1.68
Oceania	0.14	-0.70	1.76	2.24

Note: The panels present key statistics from the global distribution of air pollution by aerosols as measured by Aerosol Optical Depth (AOD). In data columns 1 and 2, we show continent-specific population-weighted means. In data columns 3 and 4, we summarise within-continent AOD distributions using relative percentile ratios. The statistics in this table are computed based on the distribution of AOD and population across cells ($1^\circ \times 1^\circ$ longitude–latitude grid) corresponding to each continent. More specifically, the interpretation of AOD is that AOD < 0.1 indicates crystal clear sky and AOD of 1 indicates very hazy conditions. For excess aerosol burden, a value of 0.5 (-0.5) indicates that a continent's AOD measure is 50 percent greater (smaller) than the global weighted mean. Finally, the P80 (P90) to P20 (P10) ratios are based on dividing the 80th (90th) percentile of the within continent AOD distribution by the 20th (10th) percentile of that distribution.